UNIVERSITY OF TARTU

FACULTY OF SCIENCE AND TECHNOLOGY

Institute of Computer Science

Cybersecurity Curriculum

Akashkumar Rajaram

Energy Harvesting in Cooperative Communications

Master's Thesis (30 ECTS)

Supervisors : Dr. Dushantha Nalin K. Jayakody

Dr. Vitaly Skachek

Tartu 2016

Energy Harvesting in Cooperative Communications

Abstract

Cooperative communications is a promising technique used to combat the multipath propagation in wireless networks. It can also extend the network coverage and provide the diversity gain by using the existing infrastructure. In practice, this is often achieved by using idle nodes in the network as relays. The multiple access relay system and parallel relay system are appealing candidates for emerging wireless cooperative networks due to bandwidth efficiency and improved power consumption.

The amplify and forward (AF) and decode and forwards (DF) protocols are basic cooperative relay protocols used over the relay channels. In this thesis, we study parallel relays in AF cooperative communication networks using QPSK signalling over the Rayleigh fast fading with additive Gaussian noise channels. The maximum ratio combining (MRC) method is employed to detect the received signals at the destination. By simulating the symbol error rate (SER) of the combined received signal at the destination, we study a trade-off between the number of relays and the quality of the communications.

The energy efficiency of a system determines its operational sustainability. Energy harvesting (EH) is a crucial technology for a variety of wireless systems that have limited access to a reliable electricity supply or recharging sources. In this thesis, the design of a multiple access relay system (MARS) using EH is considered. We assume that the sources and the relay have no embedded power supply but rechargeable energy storage devices. Thus, each node is powered by harvesting the energy from the RF signals broadcasted by an access point (AP), and it operates in store-then-cooperate (STC) mode. We simulate the link level performance by using the physical layer network coding in the presence of EH with DF protocol. The thesis presents energy harvesting schemes (EH and STC) and outage probability analysis. The schemes presented in this thesis achieve SER performance approaching that of a fixed power supply and contribute significantly to sustaining the energy in the system while maintaining a constant throughput.

Keywords: Cooperative communications, energy harvesting, parallel relay system, multiple access relay system.

CERCS : T180 Telecommunication engineering, T121 Signal processing

Energiakogumine ühiskommunikatsioonis

Kokkuvõte

Ühiskommunikatsioon on võimalik meetod lahendamaks informatsiooni levimist juhtmeta võrgus mitmikteekonna korral. See võimaldab laiendada võrgu katvust ning pakkuda võimendust kasutades olemasolevat taristut. Praktikas tehakse sedasõlmpunkte vahereleedena. Nii mitmese ligipääsuga releede süsteem kui paralleelsete releede süsteem on võimalikud kandidaadid tulevastes juhtmeta ühisvõrkudes nende ülekandekiiruse efektiivsuse ning parema energiatarbe tõttu.

Võimenda-ja-edasta (AF) ning dekodeeri-ja-edasta (DF) on peamised ühisreleede protokollid mida kasutatakse üle releekanalite. Me uurime käesolevas magistritöös paralleelseid releesid AF ühiskommunikatsiooni võrkudes kasutades QPSK signaliseerimist üle Rayleigh' kiirelt hajuva kanali koos valge aditiivse Gaussi müraga. Sihtkohas vastuvõetud signaali detekteerimiseks kasutades võrgus olevaid tegevuseta kasutatakse maksimaalse suhte ühendamise (MRC) meetodit. Mõõtes sihtkohast vastu võetud ühendsignaali sümbolite veasuhet (SER) arvutusliku simulatsiooni abil, uurime me suhet releede arvu ning kommunikatsiooni kvaliteedi vahel.

Süsteemi energeetiline efektiivsus määrab selle operatsioonilise jätkusuutlikkuse. Energiakogumise (EH) meetod on hädavajalik tehnoloogia juhtmeta süsteemides, kus on piiratud ligipääs usaldusväärsele elektritoitele ja laadimisvõimalustele. Käesolevas magistritöös uurime me mitmese ligipääsuga releede süsteeme kasutades EH tehnoloogiat. Me eeldame, et lähte- ja releesõlmedel pole ühendatud energiaallikat, kuid on taaslaetav energiatalletus. Seega, iga sõlme käivitatakse ligipääsupunkti (AP) edastatud raadiosignaalidelt kogutud energiast ning iga sõlm toimib salvesta-siis-koostööta (STC) režiimis. Me simuleerime arvutuslikult ühendusetaseme jõudlust kasutades füüsilise ühenduse võrgukodeerimist EH ja DF protokolli olemasolul. Käesolev magistritöö esitab erinevaid energiakogumise meetode (EH ja STC) ning nende katkemistõenäosusi. Esitatud skeemid saavutavad SER jõudluse, mis läheneb püsiva toiteallikaga jõudlusele ning laiendab oluliselt süsteemi energiapüsivust, samas säilitades pidevat läbilaskejõudlust.

Märksõnad: ühiskommunikatsioon, energiakogumine, paralleelsete releede süsteem, mitmese ligipääsuga releede süsteem.

CERCS : T180 telekommunikatsioonitehnoloogia, T121 signaalitöötlus.

Acknowledgment

The thesis work has been carried out at the Coding and Information Transmission Group, Institute of Computer Science, University of Tartu as part of Cybersecurity Curriculum. This thesis is presented at Institute of Computer Science at University of Tartu for the degree requirements of Master of Science in Cyber Security at Tallinn University of Technology. The thesis work was conducted under the guidance of Dr. Nalin Jayakody and Dr. Vitaly Skachek.

I express my sincere gratitude to Dr. Nalin Jayakody and Dr.Vitaly Skachek for their extended supervision, feedback and reviews throughout the thesis. I am thankful to Tallinn University of Technology and University of Tartu for providing me this opportunity to pursue my master's degree.

I am thankful for Ivo, Amin, Waheed, Satish, Suresh, Karthik kumar, my family friends, Estonians and many good people whom I met in my life.

I express my love and affection to my beloved parents and sisters for their moral support and motivation throughout my life.

This work is supported (in part) by the Norwegian-Estonian Research Cooperation Programme through the grant EMP133, by the Estonian Research Council through the research grants PUT405 and IUT2-1.

Akashkumar Rajaram,
Tartu, 19^{th} May, 2016.

Contents

List of Figures

1. Introduction

1.1 Wireless communication network

Wireless cooperative communications is an effective method of extending the network coverage or providing the diversity gain using existing infrastructure. In practice, this is often achieved by using idle nodes in the network as relays to forward the signals from the source to the destination [32]. Wireless communication network (WCN) is a collection of nodes and wireless links. In WCN the packets are routed from sources to destinations and links are represented by channels. Channel fading is a natural phenomenon occurring due to multipath propagation of a signal. It is one of the main challenges in WCN. Channel fading causes the attenuation of the signal which degrades the quality of information passed over the WCN in addition to signal distortion caused by the noise.

To overcome the effects of channel fading we could use diversity scheme. Diversity scheme improves the signal reliability by comparing the different versions of the signal received from the source through independent channels.

Additive white Gaussian noise (AWGN) is a basic noise model used in the area of the information theory to mimic the effect of many random processes that occur in nature. AWGN characteristics:

- Additive - Because it is added to any noise that might be intrinsic to the information system.
- White - It has uniform power across the frequency band for the information system and

has uniform emissions at all frequencies in the visible spectrum.

- Gaussian - Because it has a normal distribution in the time domain with an average time domain value of zero.

Phase-shift keying (PSK) is a digital modulation scheme that modulates data signal by changing the phase of the carrier sine wave. Binary Phase-shift keying (BPSK) is a simplistic PSK scheme in which carrier wave is modulated at (180, 0) degrees for each change in the binary state. The general form for BPSK:

$$s_k(t) = \sqrt{\frac{2E_s}{T}}\cos(2\pi f t + \pi(1-q)), \quad q = (0,1),$$

where f is the frequency of the carrier-wave. E_s and T are energy per bit and bit duration, respectively.

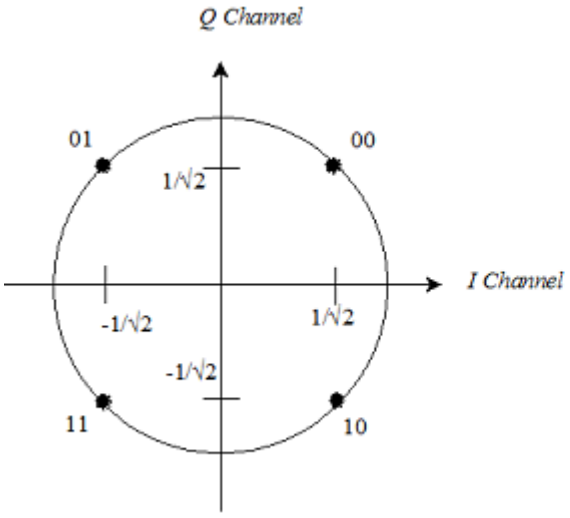

$b(n), b(n+1)$	I	Q
00	$1/\sqrt{2}$	$1/\sqrt{2}$
01	$1/\sqrt{2}$	$-1/\sqrt{2}$
10	$-1/\sqrt{2}$	$1/\sqrt{2}$
11	$-1/\sqrt{2}$	$-1/\sqrt{2}$

Figure 1.1: QPSK Constellation figure with phase shifts of (45, 135, 225, 315 degrees) and its representation in the vector domain

Quadrature Phase Shift Keying (QPSK) is a PSK scheme in which two bits are modulated at once, selecting one of four possible carrier phase shifts as in Fig. 1.1. The corresponding angles are 45, 135, 225, 315 degrees. QPSK increases the capacity of the carrier wave by carrying twice as much information as BPSK using the same bandwidth. The general form for QPSK in terms of the sine and cosine waves as per constellation diagram.

$$s_k(t) = \sqrt{\frac{2E_s}{T}}\cos(2\pi f t + (2q-1)\frac{\pi}{4}), \quad q = 1,2,3,4.$$

Pairs of bits $b(n)$ and $b(n+1)$ are mapped to complex-valued modulation symbols $S = I + jQ$, where $j = \sqrt{-1}$. In this thesis we restrict our attention to QPSK signalling.

1.1.1 Rayleigh fading channel

The Rayleigh fading is caused by multipath reception. The basic model of Rayleigh fading assumes a received multipath signal to consist of a (theoretically infinitely) large number of reflected waves with independent and identically distributed inphase and quadrature amplitudes. So when considering a mobile antenna, which receives a large number, say N, reflected and scattered waves. Because of wave cancellation effects, the instantaneous received power seen by a moving antenna becomes a random variable, dependent on the location of the antenna.

In probability theory and statistics, the Rayleigh distribution is a continuous probability distribution for positive-valued random variables. A Rayleigh distribution is often observed when the overall magnitude of a vector is related to its directional components. An example of the distribution arises in the case of random complex numbers whose real and imaginary components are independently and identically distributed (i.i.d.) Gaussian with equal variance and zero mean. In that case, the absolute value of the complex number is Rayleigh-distributed.

Let X and Y be symmetric random variables.

Define Z as $Z = X + jY$, where Z is complex Gaussian distribution. The statistics of a circularly symmetric complex Gaussian random variable is completely specified by the variance is

$$\sigma^2 = \mathbb{E}[Z^2], \text{ where } \mathbb{E} \text{ is expectation.}$$

The Phase θ is uniformly distributed from [0,2π], $\quad \theta = \tan\frac{X}{Y}$.
In Fig. 1.2, the area $dxdy$ is Cartesian coordinate form is equal to the area $zdzd\theta$ in the polar coordinate form. Probability distribution functions (PDF) for Z and θ are given as

$$p(Z) = \frac{Z}{\sigma^2}e^{\frac{-Z}{2\sigma^2}}, Z \geq 0 \text{ and } p(\theta) = \frac{1}{2\pi}, \quad \pi \leq \theta \leq \pi.$$

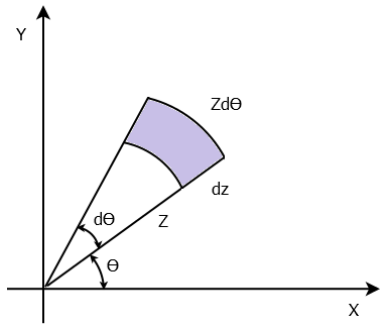

Figure 1.2: Cartesian coordinate to polar coordinate

1.1.2 Wireless channel capacity and outage probability

Channel capacity is derived for a various communication scenarios by Claude E. Shannon [1]. It characterizes the maximum information rate for which reliable communications is possible.

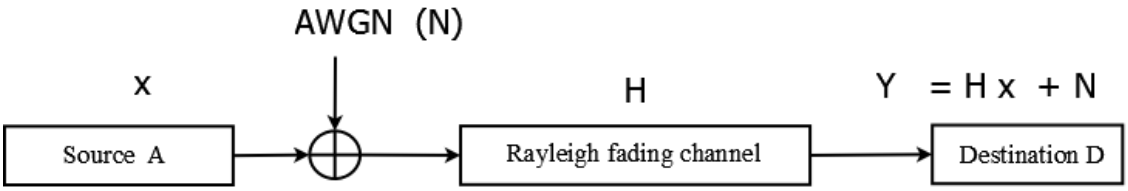

Figure 1.3: Rayleigh fading channel with AWGN and power constraint

The received signal at destination D from source A, $Y = \sqrt{P}Hx + N$,

In case of Rayleigh slow fading, the channel capacity is given as

$$C = \log_2(1 + |H|^2 SNR),$$

$$SNR = \frac{\text{Power constraint of signal}}{\text{Power constraint of noise}} = \frac{\mathbb{E}[(\sqrt{P})^2]}{\mathbb{E}[N^2]} = \frac{\mathbb{E}[(\sqrt{P})^2]}{\mathbb{E}[N^2]} = \frac{P}{N_0},$$

where H is channel fading coefficient and SNR is transmitting signal to noise ratio. Here, P is the power constraint of signal and N_0 is noise spectral density power. A fading channel is called fast fading channel if the channel impulse change is rapid i.e. high variation in the mean value of the signal. A fading channel is called slow fading channel if the channel impulse change is slow i.e. slow variation in the mean value of the signal.

The difference between channel capacity of the slow fading and fast fading channel is the coherence time T_c of the channel with respect to a sampling period, T_s.

In slow fading, $T_c >> T_s$. So the channel remains constant over the transmission and the chan-

nel does not have multiple sub-channels.

In fast fading, $T_c < T_s$, so the channel fades fast and the channel has multiple sub channels. Lets the sub channel H_g, where g is the total number of sub channel.

$$C(H;SNR) = \sum_{n=0}^{N_c-1}(\log_2(1+|H|^2 SNR)).$$

In the slow fading, the channel remains constant over the transmission duration of the codeword. If the codeword length spans several coherence periods, then time diversity is achieved and the outage probability improves. Capacity of Rayleigh fast fading channel is given as

$$C(H;SNR) = \mathbb{E}(\log_2(1+|H|^2 SNR)).$$

Outage probability P_o of wireless communication channel depends the channel capacity C and target rate R. If the channel capacity is less than the target rate then outage event occurs.

$$\begin{aligned} P_o &= Pr(C(H;SNR) < R) \\ &= Pr(\mathbb{E}(\log_2(1+|H|^2 SNR)) < R) \end{aligned}$$

$$P_o = Pr(C(H;SNR) < R) = Pr(R_i < R),$$

where is an $|H|^2$ follows exponential random variable,

$$Pr(R_i) = \frac{1}{SNR}\text{EXP}\Big(\frac{-R_i}{SNR}\Big),$$

$$Pr(R_i < R) = \int_0^R \frac{1}{SNR}\text{EXP}\Big(\frac{-R_i}{SNR}\Big).dR_i,$$

$$P_o = 1 - \text{Exp}(-(R/SNR)),$$

where P_o shows the reliability of channel for sending information at target rate R.

1.2 Cooperative wireless communication

In cooperative communication, cooperation using the classical three node system with a relay is introduced in [5]. The capacity of non-fading relay channels with additive white Gaussian noise

and lower and upper bounds on the capacity is derived in [27]. Later, several coding strategies for relay channel with the ergodic capacity of the channel under certain criteria are proposed in [28]. Cooperative communication is based on the user cooperation and cooperative diversity of the network nodes. User cooperation is the resource sharing among multiple devices present in the WCN, as it is introduced in [6],[7]. The cooperative diversity is a multiple antenna technique for combating multipath fading in WCN. The cooperative diversity of multiuser environment is studied in [8] and [9].

In user cooperation a new path arises in between source to destination when a new node (relay) is introduced. The communication nodes work together to deliver their signal by relaying information from the source. An independent copy of the data is generated in the relaying process and sent to destination. The processing of multiple independent copies of the signal at the destination reduces the probability of error. Acquired diversity improves channel reliability and saves resources [26] [27].

Cooperative communications protocols are divided into two main categories: fixed relaying schemes and adaptive relaying schemes. In fixed relaying, the channel resources are divided between the source and the relay in a fixed manner. Further fixed relaying scheme can be categorized based on their approaches into Fixed Amplify and Forward protocol (AF) and Fixed Decode and Forward (DF) protocol. AF and DF protocols are first introduced in [26] and [3]. The cooperative diversity and outage behaviour of relay DF and AF protocols are also analysed in [26].

In AF relaying protocol, the relay simply scales the received signal and transmits an amplified version of the received signal to the destination. In DF the protocol, the relay decodes, re-encodes, and retransmits the received signal to the destination.

Multiple access relay system (MARS) is a model in which multiple sources are allowed to transmit signals to a single relay. MARS is first introduced as a multiple access channel in [11] and further decoding techniques with analysis of achievable rates are proposed in [11] and bounds on the total capacity of the channel are derived in [12].

In this thesis, we study three types of relay networks as depicted in Fig. 1.4.

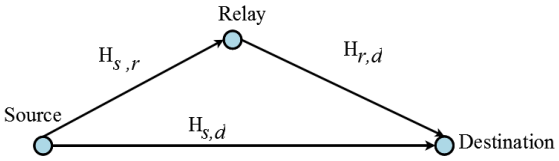

(a) single relay system,

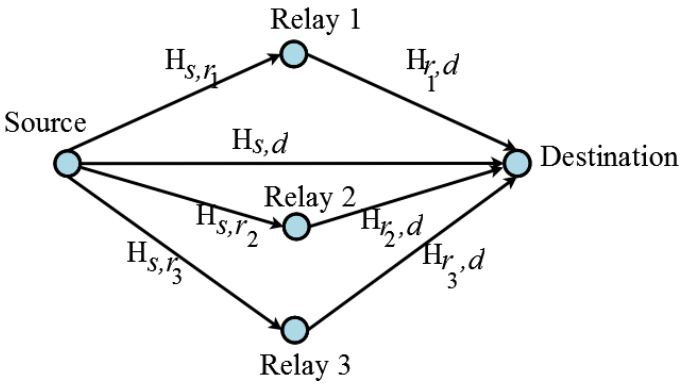

(b) Multiple relay system,

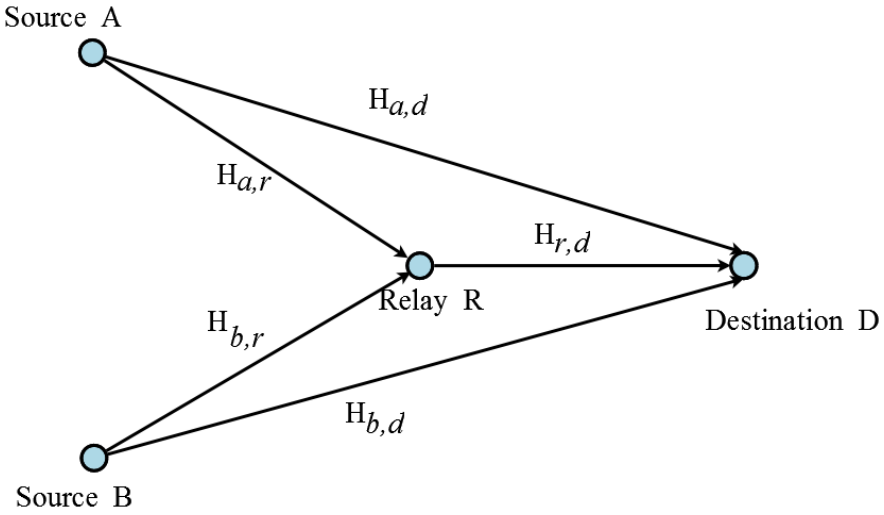

(c) Multiple access relay system.

Figure 1.4: Cooperative networks

- In a single relay system, source transmits signal to the relay. The destination receives two versions of signals from source, one is directly transmission from source and the other one is through a relay. There by destination has the signal with cooperative diversity of order 2.
- In multiple relay system, source send signal to three relays. Here destination receives four versions of signals. One version is directly from the source transmission and other 3 versions are from the relay transmissions. Destination has the signal with cooperative diversity of order 4.
- In multiple access relay system, two sources send signals to a single relay. Relay receives two signals and it can transmits the signals separately or it can transmit signals as a com-

bined signal to the destination. Here destination has 2 different signals with diversity order of 2.

1.3 Log likelihood ratio

The likelihood of a set of parameter values, θ, given outcomes x, is equal to the probability of those observed outcomes given those parameter values [13]. The natural logarithm of this function is log likelihood function.

By using Neyman−Pearson lemma function [14], we conduct the LLR for a SISO system with BPSK and QPSK modulation. The derivations for a system model with BPSK signal and QPSK signal given as follows.

From the Fig. 1.3, the received signal is Y at destination in a point to point Rayleigh fading channel is

$$Y = \sqrt{P}Hx + N. \tag{1.1}$$

LLR of Y for BPSK modulation,

$$LLR_Y = \log\left(\frac{Pr(x=1|Y)}{Pr(x=-1|Y)}\right), \tag{1.2}$$

where N is $2\sigma^2$.

By using Gausian distribution on (1.2),

$$\begin{aligned} Pr(x=1|Y) &= \frac{1}{\sqrt{2\pi\sigma^2}} e^{\frac{-(Y-\sqrt{P}H)}{2\sigma^2}^2}, \\ Pr(x=-1|Y) &= \frac{1}{\sqrt{2\pi\sigma^2}} e^{\frac{-(Y+\sqrt{P}H)}{2\sigma^2}^2}. \end{aligned} \tag{1.3}$$

By substituting (1.3) in (1.2) we obtain,

$$LLR_Y = \log\left(\frac{e^{\frac{-(Y-\sqrt{P}H)^2}{2\sigma^2}}}{e^{\frac{-(Y+\sqrt{P}H)^2}{2\sigma^2}}}\right), \tag{1.4}$$

$$LLR_Y = \left(\frac{-(Y - \sqrt{P}H)^2}{2\sigma^2} - \frac{-(Y + \sqrt{P}H)^2}{2\sigma^2} \right), \tag{1.5}$$

Simplifying (1.5) gives LLR of BPSK signal in Rayleigh fading channel as

$$LLR_Y = \frac{2\sqrt{P}HY}{\sigma^2} \tag{1.6}$$

LLR of the received signal is Y with QPSK modulation is derived as follows. a^* is represented as the conjugate of complex number a.

$$YH^* = \sqrt{P}HH^*x + (NH^*), \tag{1.7}$$

By simplifying we obtain,

$$LLR_Y = \frac{2\sqrt{P}|H|^2Y}{\sigma^2}, \tag{1.8}$$

where $\sigma^2|H^*|^2$ is the variance of NH^*.

1.4 Physical layer network coding

The concept of physical-layer network coding (PLNC) was introduced by Zhang in 2006 [15]. Algebraic superposition of channel codes over finite fields was proposed by Xiao in [16] for efficient use of resource by avoiding the excess resource allocation in the previous designs.

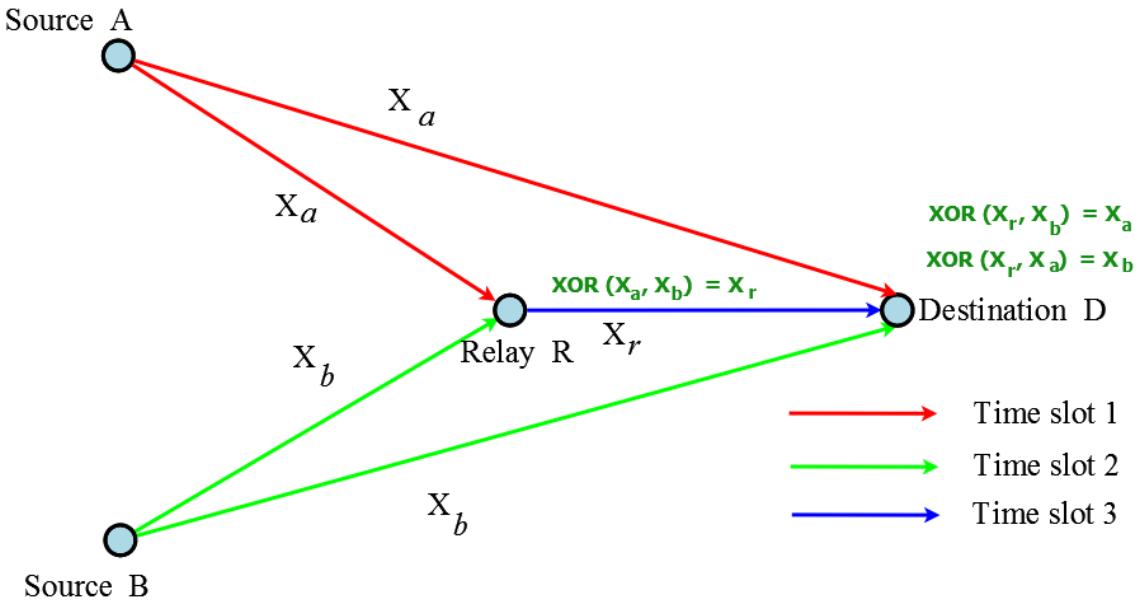

(a) PLNC with three time slots.

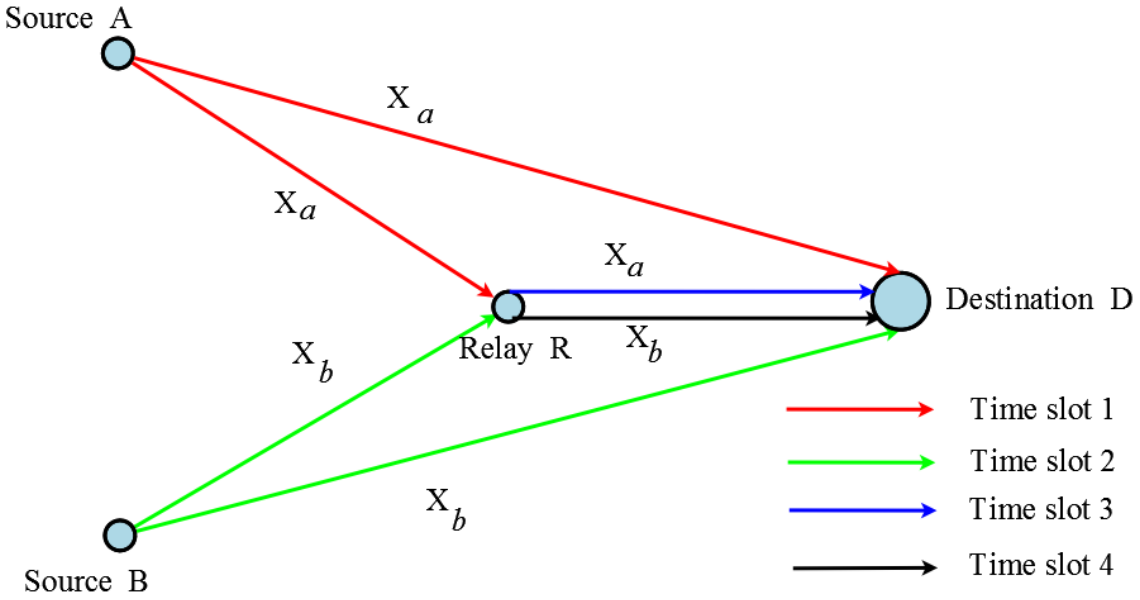

(b) Forwarding with four time slots.

Figure 1.5: Comparison of PLNC and Forwarding for MARS.

PLNC is a promising technique to increase the throughput of a wireless network, i.e. the PLNC is used in wireless network to reduce the time slots in between nodes communicating via relay. This concept utilizes the natural phenomena of superimposing electromagnetic (EM) waves (radio waves from an unintended transmitter considered interference for the intended signal can be used as an advantage). Throughput is defined as the number of bits, excluding control bits,

successfully transmitted in a time slot over a communication channel. Thus, the increase in throughput effectively reduces the energy consumption during the transmission. The mechanism of PLNC is to perform a XOR-like operation to the signal from the superimposed EM, which is formed by the signal of different nodes sent over the relay. The process to deducing XOR-like product in the PLNC from the superimposed EM is called PLNC mapping [21].

Fig. 1.5 explains the comparison of PLNC and forwarding for MARS. In PLNC we have three time slots and in forwarding we have 4 times slots. In time slot 1 and time slot 2 both the sources A and B transmits signals X and X_b to relay R respectively.

In time slot 3 relay receives the signals from both sources and by using PLNC, superimposed EM signal X_r is obtained by addition of X_a and X_b is transmitted to the destination D. Destination D performs network decoding operation to separates the signals X_a and X_b by using XOR operation on X_r. Due to use of PLNC in the system the number of time slots are reduced to 3 instead of 4 compared to forwarding.

1.5 Energy harvesting in wireless communication network

Energy harvesting in wireless communication network is a method to increase energy efficiency of network. It is one of the key focus area for the future generation of wireless communications. The increasing number of electronic devices to support the growth of wireless data services is a reason for energy harvesting in electronic devices.

In many practical communication scenarios without access to natural light or wind sources, conventional energy harvesting techniques are not applicable, which motivates the concept of wireless RF energy harvesting. Radio Frequency (RF) energy harvesting and transfer technique, has recently regarded as a promising avenue for power energy-constrainted wireless networks (see [17, 18] and references therein). RF energy harvesting typically refers to the capability of wireless devices to convert the received RF signals into usable energy, while the RF energy transfer refers to the technique of an energy transmitter to deliver energy in wireless fashion to the devices by leveraging the far-field radiative properties of electromagnetic waves. Traditionally, the wireless terminals are normally powered by the batteries with limited operation duration.

Frequent battery recharging/replacement is inconvenient due to huge numbers of devices in use, hazardous for the devices located in toxic environment, or even impracticable in many applications, e.g., medical devices. In these scenarios, the RF energy harvesting technique becomes an attractive approach to charge the batteries of wireless devices [35]. The feasibility of this technique has been experimentally demonstrated by prototypes, such as [20]. This result in significant gains in terms of spectral efficiency, time delay, and the energy consumption. There are two types of harvesting, ambient and dedicated RF harvesting based on the transmitter. If the transmitter does not transmits a dedicated RF signal and receiver utilize the ambient RF signals available then it is ambient RF harvesting. Ambient RF energy harvesting is uncontrollable and unpredictable but its more adaptable [22],[23] compared to dedicated RF energy harvesting [24],[25].

Rectenna is the antenna used to harvest RF energy and rectifies microwave energy to DC electricity. The conversion efficiency of rectenna is the measure of RF power received by the antenna to DC power converted by the rectenna.

1.6 Contributions

The main contributions of this thesis are:

1 Performance analysis of parallel relay network with AF protocol and multiple relays. We show by simulations that the SNR gain improves with the increase in the number of relays. We also show that the relative SNR gain decreases with increase in a number of relays, thereby finding a nearly-optimal number of relays for combating multipath propagation.

2 Implementation of PLNC for three models: MARS with direct power supply, MARS with the EH scheme and MARS with improved EH scheme called *store-then-cooperate* scheme. We perform simulations of performance of these schemes. The simulations show the performance improvements offered by the STC scheme.

3 Improvement of EH by using a battery at each node and analysis of the corresponding system. The proposed STC scheme improves the outage probability of the system when

compared to EH scheme. The outage probability of the system with STC is similar to that of the system with direct power supply. Finally, we conclude the chapter by introducing a dynamic switch.

2. Performance Analysis of Parallel Relay Network[1]

2.1 System model

In this section we adapt fixed AF protocol for QPSK signalling over Rayleigh fast fading channel with additive white Gaussian noise in a parallel relay network (PRN). All the nodes in the model consist of a single antenna and a single receiver and operates in half duplex mode.

In PRN, the signal propagates from the source through parallel relay paths to the destination and the destination combines the signals received through different paths. The main advantage of PRN is that the destination makes use of the diversity gain attained by combining multiple reception from the relay and the source [28], [29]. Diversity is a property of improving the quality of reception by using several communication paths. Maximum ratio combining (MRC) is a diversity combining method for combining all the signals in a co-phased and weighted manner in order to have highest achievable SNR at the receiver. In MRC, all the branches are used simultaneously. Each of the branch signals is weighted with a gain factor proportional to its own SNR.

Basic AF relaying protocol: In this model we consider a network with a source, a destination and a single relay as it is shown in Fig. 2.1. In a basic fixed AF relaying protocol, there are two phases. In the first phase the source transmits a signal to the relay and the destination in the

[1]The material in this section is based on the work done in the course, MTAT.03.309 - Special Assignment in Wireless Communication (University of Tartu)

same time slot. In the second phase the relay amplifies the signal received from the source and retransmits to the destination. Then destination uses MRC to combine the received signals in order to achieve the diversity gain.

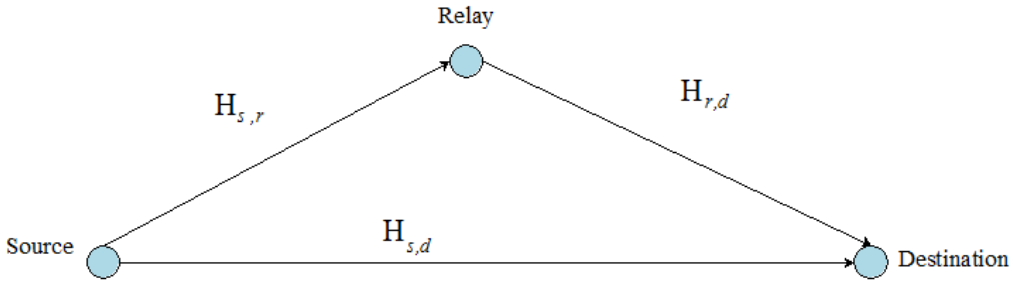

Figure 2.1: Single fixed amplify and forward cooperation network model.

Phase 1:

The received signal at the destination (from the source) is :

$$Y_{s,d} = \sqrt{P_0} H_{s,d} x + N_{s,d}, \tag{2.1}$$

where P_0 is the transmitted power at Phase 1. The received signal at the relay (from the source) is :

$$Y_{s,r} = \sqrt{P_0} H_{s,r} x + N_{s,r}. \tag{2.2}$$

Here $H_{s,r}$ and $H_{s,d}$ are the channel fading coefficients from the source to the relay and the source to the destination, respectively. They are modelled as Rayleigh flat fading channels. The terms $N_{s,r}$ and $N_{s,d}$ denote the additive white Gaussian noise with zero mean. We use N_0 to denote noise spectral density power which is modelled as zero mean complex Gaussian random variable.

Phase 2:

Channel gain of the received signal $Y_{s,r}$ and noise are amplified in the relay and the amplification factor is denoted by β. The co-efficient β maintain a constant average transmit power at the

relay and equal P_1,

$$\mathbb{E}[\beta Y_{s,r}] \leq P_1.$$

$$\sqrt{P_1} = \beta Y_{s,r},$$

$$\begin{aligned}\beta^2 &= \frac{\mathbb{E}[(\sqrt{P_1})^2]}{\mathbb{E}[Y_{s,r}^2]} \\ &= \frac{\mathbb{E}[(\sqrt{P_1})^2]}{\mathbb{E}[(H_{s,r}x\sqrt{P_0} + N_{s,r})^2]} \\ &= \frac{\mathbb{E}[(\sqrt{P_1})^2]}{\mathbb{E}[H_{s,r}^2 P_0 x^2 + N_{s,r}^2 + 2N_{s,r}H_{s,r}xP_0]} \\ &= \frac{\mathbb{E}[(\sqrt{P_1})^2]}{\mathbb{E}[H_{s,r}^2 P_0 x^2] + \mathbb{E}[N_{s,r}^2] + \mathbb{E}[2N_{s,r}H_{s,r}xP_0]}.\end{aligned}$$

The noise term $N_{s,r}$ and the signal x appear to be i.i.d. and therefore the term $\mathbb{E}[2N_{s,r}H_{s,r}xP_0]$ is neglected.

$$\beta = \frac{\sqrt{P_1}}{\sqrt{P_0|H_{s,r}|^2 + N_0}} \tag{2.3}$$

The relay amplifies both the received signal and the noise and forwards the amplified signal to the destination. The received signal at the destination is given by

$$Y_{r,d} = \beta H_{r,d} Y_{s,r} + N_{r,d}. \tag{2.4}$$

The transmit power is set as $P_0 = P/2$ and $P_1 = P/2$, where P is the transmit power at source, P_0 and P_1 are the values of the transmit power at Phase 1 and Phase 2, respectively. Here, $N_{r,d}$ and $H_{r,d}$ denote the AWGN term of the source to the destination channel and the channel fading coefficient of the source to the destination channel, respectively.

Parallel relay AF protocol:

Consider the system model with parallel relays as in Fig. 2.2 . Let N be the number of the relays in the system.

Phase 1:

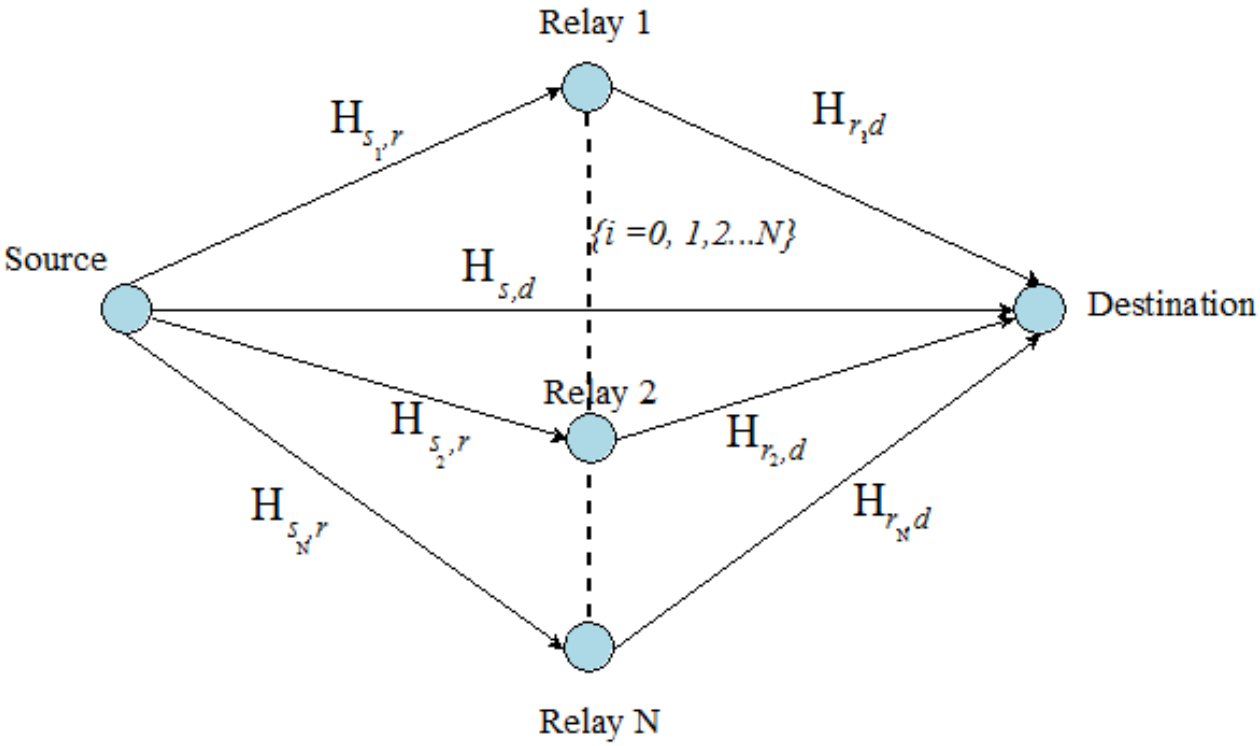

Figure 2.2: Parallel relay AF protocol model.

The received signal at the destination (from the source) is :

$$Y_{s,d} = \sqrt{P_0} H_{s,d} x + N_{s,d}, \tag{2.5}$$

The received signal at the relay (from the source) is :

$$Y_{s,r_i} = \sqrt{P_0} H_{s,r_i} x + N_{s,r_i}. \tag{2.6}$$

Phase 2:

The received signal Y_{s,r_i} is amplified in the relay and this can be termed as amplification factor β_i :

$$\beta_i = \frac{\sqrt{P_i}}{\sqrt{P_0 |H_{s,r_i}|^2 + N_0}}, \tag{2.7}$$

The received signal at the destination is given as :

$$Y_{r_i,d} = \beta H_{r_i,d} Y_{s,r_i} + N_{r_i,d}, \tag{2.8}$$

where the relays are indexed by $i = 1,2,...N$, and P_0 is the transmit power at the source. Here, $N_{s,d}$, N_{s,r_i} and $N_{r_i,d}$ denote AWGN of source to destination, source to i th relay and i th relay to destination channels, respectively. Additionally, $H_{s,d}$, H_{s,r_i} and $H_{r_i,d}$ are the channel fading coefficients from the source to the destination, source to i th relay and i th relay to destination, respectively. Power constrain at the i th relay is P_i.
We set transmit powers to be

$$P_0 = P/2, \qquad P_i = P_0/i, \tag{2.9}$$

where P is the total power P_0 is the power in phase 1 and P_i is the power in phase 2.

2.2 Symbol error rate analysis

The symbol error rate (SER) can be found by estimating over all SNR values in the AF protocol. By using MRC the signal is combined at the destination as

$$y = \alpha_1 . Y_{s,d} + \alpha_2 . Y_{r,d}, \tag{2.10}$$

where

$$\alpha_1 = \frac{\sqrt{P} H^*_{s,d}}{N_0} \qquad \text{and} \qquad \alpha_2 = \frac{\sqrt{\left(\frac{P}{P|H_{s,r}|^2+N_0}\right)} P H^*_{s,r} H^*_{r,d}}{(\frac{P|H_{r,d}|^2}{P|H_{s,r}|^2+N_0} + 1) N_0}.$$

Here, y is the combined signal received at the destination, and α_1 and α_2 are combining factors for the received signals $Y_{s,d}$ and $Y_{r,d}$, respectively.

Asymptotically tight approximation:

Asymptotically tight approximation is provided to understand the asymptotic performance of the systems and to approximately closer to the actual value, in which the approximation of the

error probability is asymptotically tight at high SNR as in [31, (5.71)],

$$\wp_{PSK} = \frac{1}{\pi}\int_0^{\frac{(M-1)\pi}{M}} \frac{1}{1+\frac{b_{PSK}}{\beta_0 \sin^2\theta}}\Bigg\{\frac{(\beta_1-\beta_2)^2+(\beta_1-\beta_2).\frac{b_{PSK}}{\beta_0\sin^2\theta}}{\Delta^2} + \frac{2\beta_1\beta_2 b_{PSK}}{\Delta^3\sin^2\theta}\ln\frac{\left(\beta_1-\beta_2+\frac{b_{PSK}}{\beta_0\sin^2\theta}+\Delta^2\right)}{4\beta_1\beta_2}\Bigg\}d\theta, \tag{2.11}$$

in which $\beta_0 = N_0/(P_1\delta^2_{s,d})$, $\beta_1 = N_0/(P_1\delta^2_{s,r})$, $\beta_2 = N_0/(P_1\delta^2_{r,d})$ and $\Delta^2 = (\beta_1-\beta_2)^2+2(\beta_1+\beta_2)s+s^2$ with $s = \frac{b_{PSK}}{\beta_0\sin^2\theta}$ and $b_{PSK} = sin^2(\pi/M)$ for M-PSK modulation.

The notations denote the , $\delta_{s,d},\delta_{s,r},\delta_{r,d}$ the channel gain variance of the source to the destination, the source to a relay and a relay to the destination channels, respectively.

A asymptotically tight approximation for the SER formulations can be provided when all of the channel links are available, i. e., $\delta_{s,d}\neq 0,\delta_{s,r}\neq 0,\delta_{r,d}\neq 0$ [31].

By using equation as in [31, (6.86)],

$$\wp_N \approx \frac{BN_0^{(N+1)}}{b^{(N+1)}}.\frac{1}{P_1\delta^2_{s,d}}\prod_{i=1}^{N}\left(\frac{1}{P_1\delta^2_{s,r_i}}+\frac{1}{P_2\delta^2_{r_i,d}}\right), \tag{2.12}$$

where $B = \frac{3(M-1)}{8M}+\frac{\sin\frac{2M}{\pi}}{4\pi}-\frac{\sin\frac{4M}{\pi}}{32\pi}$ and $b = b_{PSK}$ and the number of the relays is given as i, $i = 1,2,...,N$. The upper index $(N+1)$ next to N_0 and b means that the number of relays in the system is N.

For single relay amplify and forward as in (2.1),the number of the relays $N = 1$. By using (2.12) we obtain

$$\wp_1 \approx \frac{BN_0^{(2)}}{b^{(2)}}\frac{1}{P_1\delta^2_{s,d}}\left(\frac{1}{P_1\delta^2_{s,r}}+\frac{1}{P_2\delta^2_{r,d}}\right). \tag{2.13}$$

Parallel relay AF protocol:

Similarly, for multiple relay case by using (2.2) and (2.10), we obtain

$$\alpha_1 = \frac{\sqrt{P}H^*_{s,d}}{N_0}, \qquad \alpha_i = \frac{\sqrt{\frac{P}{P|H_{s,r_i}|^2+N_0}}}{\left(\frac{P|H_{r_i,d}|^2}{P|H_{s,r_i}|^2+N_0}+1\right)N_0} PH^*_{s,r_i}H^*_{r_i,d}, \tag{2.14}$$

$$y = \alpha_1 Y_{s,d} + \sum_{i=0}^{N} \alpha_i Y_{r_i,d}. \tag{2.15}$$

Asymptotically tight approximation of the symbol error probability $\wp_N$ to N parallel relay is given in (2.12).

2.3 Simulation results

Number of the input symbols per time unit is 10^6 and the SNR ranges between 0 to 36 dB. We consider Rayleigh fast fading channel with AWGN noise.

We present the simulation results of the two systems used over Rayleigh fast fading channel with AWGN. The purpose of the simulations is to analyze the performance of the system with AF cooperation and the system with no cooperation.

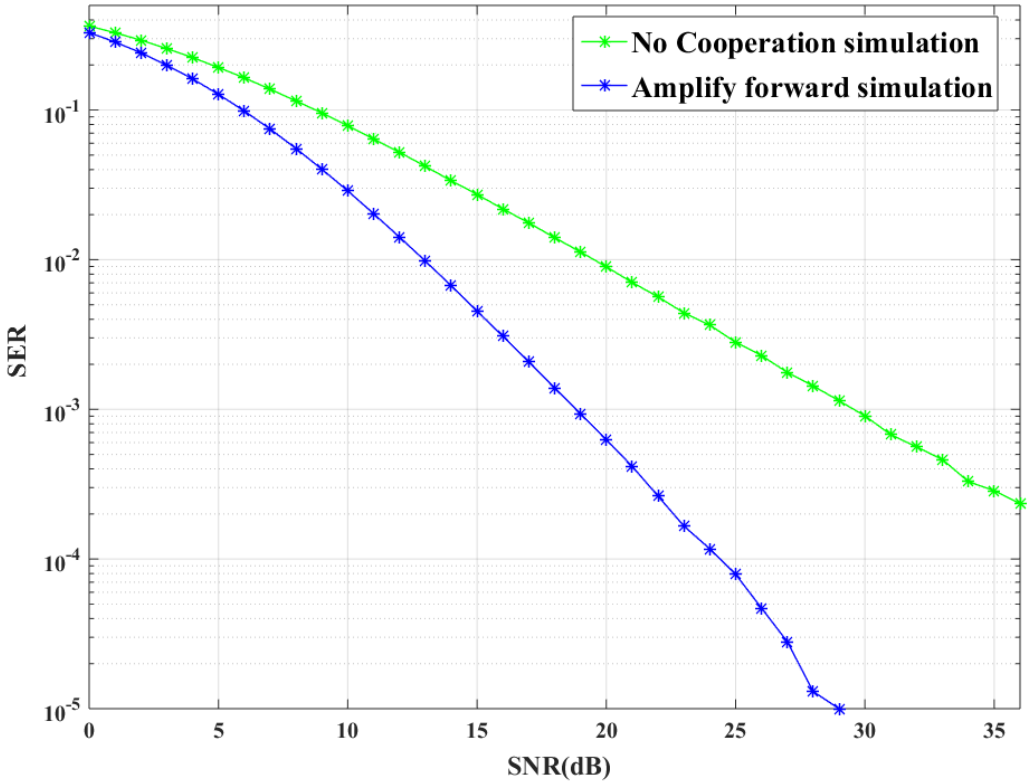

Figure 2.3: Comparison of the system with AF cooperation and the system with no cooperation.

In Fig. 2.3, we obseve that the SER value of AF cooperation network is lower than no-cooperation network with respect to their SNR because AF network utilizes the diversity gain at the destination. The analysis of no-cooperation and AF cooperation curves in Fig. 2.3 shows that SER value is lower in AF cooperation scenario compared to no cooperation system.

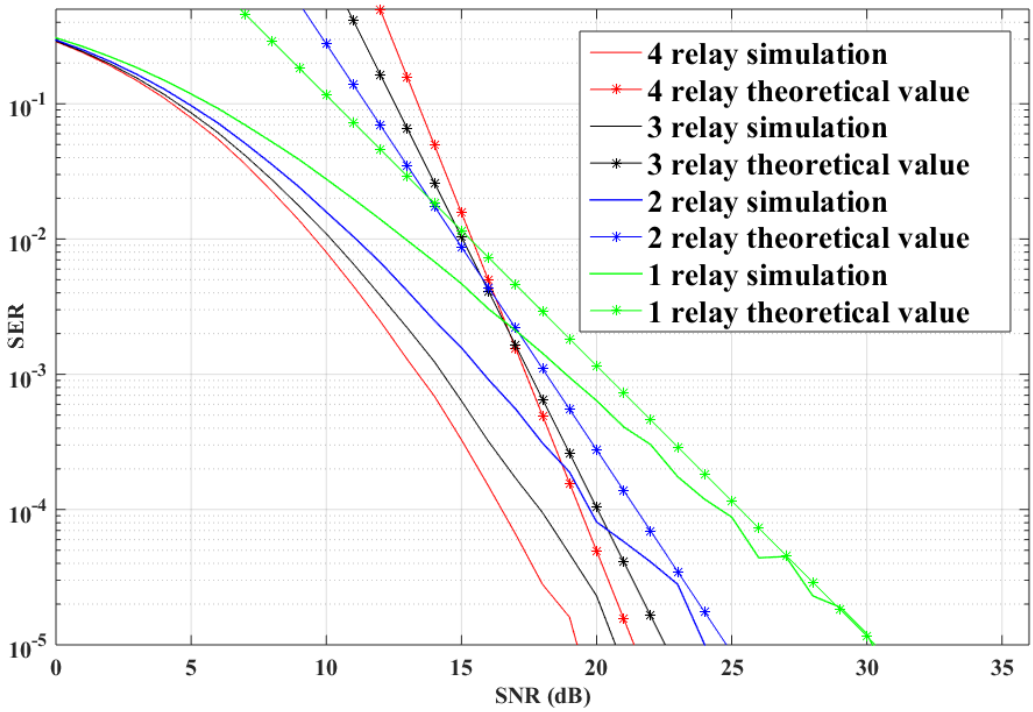

Figure 2.4: Parallel amplify and forward cooperation network model with 1, 2, 3 and 4 parallel relays.

In Fig. 2.4, we demonstrate the performance of the relay system with 1, 2, 3 and 4 parallel relays, respectively. The performance of the system with 1 and 2 relays is comparable to the theoretical approximation of (2.12) at high SNR. By contrary, the performance of the system with 3 and 4 relays does not match the theoretical estimate even at high SNR but the gap between simulated values decreases as SNR grows.

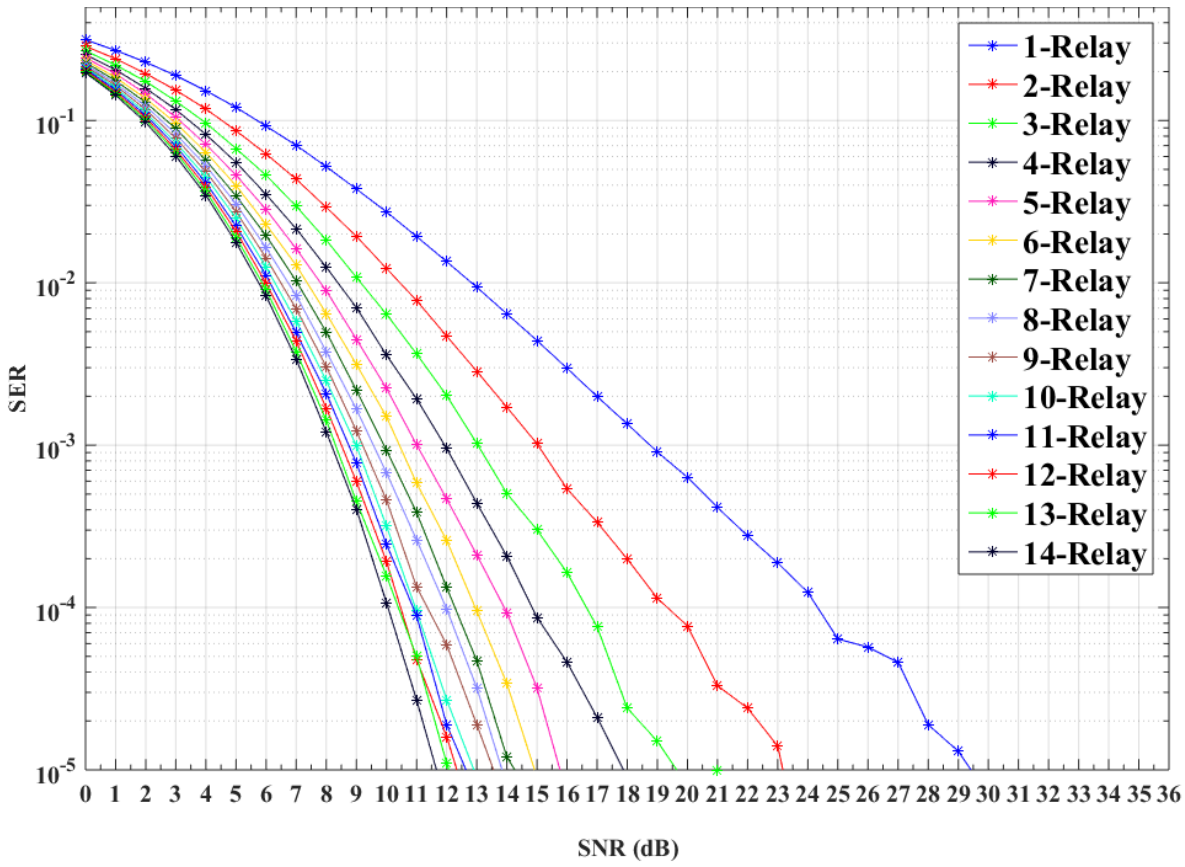

Figure 2.5: Comparison of parallel relay AF cooperation network model to find the channel gain pattern with addition of every new relay to the network.

In Fig. 2.5, we demonstrate 14 different relay networks where the number of relays varies from 1 to 14 respectively. We observe that the performance improves with the increase in a number of relays in the network due to addition of diversity gain for every extra relay in the destination. Moreover, the performance improves with increase in overall SNR value. The relative SNR gain between the relay system decreases with increase in a number of relays.

The following table summarizes our results.

Pair number.	No of relays used in adjacent curves.	SNR value of adjacent curves (dB)	Relative SNR gain (dB)
1	1 - 2	29.5 - 23.2	6.3
2	2 - 3	23.2 - 19.5	3.8
3	3 - 4	19.5 - 18.0	1.5
4	4 - 5	18.0 - 15.8	2.2
5	5 - 6	15.8 - 15.0	0.8
6	6 - 7	15.0 - 14.3	0.7
7	7 - 8	14.3 - 13.9	0.4
8	8 - 9	13.9 - 13.5	0.4
9	9 - 10	13.5 - 13.0	0.5
10	10 -11	13.0 - 12.8	0.2
11	11- 12	12.8 - 12.3	0.5
12	12 - 13	12.3 - 12.0	0.3
13	13 - 14	12.0 - 11.8	0.3

Table 2.1: The results in Fig. 2.5 shows the relative gain for the parallel relay system with the addition of each relay at SER = 10^{-5}

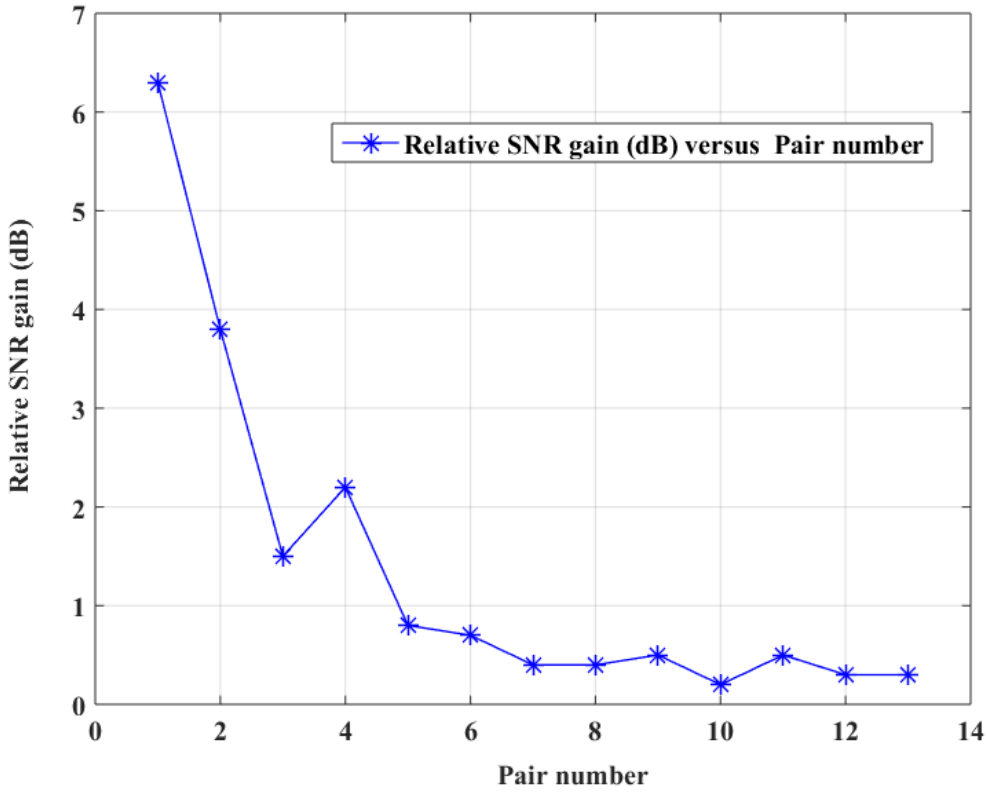

Figure 2.6: Adjacent relay pair number versus relative SNR gain (dB) as observed from Table 2.1.

From Table 2.1 and Fig. 2.6, we observe the drastic decrease in the channel gain between two adjacent relay curves from 1-2 relays to 5-6 relays. From 6-7 relays to 13-14 relays the channel gain gradually decreases and tends to saturate below 0.5 decibel. This indicates that in the system with more than 7 relays a gain less than 0.5 decibel for each additional relay is expected. We observe that the SNR gain decreases for a larger number of relays. We also note the SNR gain saturation phenomenon when the number of the relays exceeds 7.

3. Wireless Energy Harvesting in Cooperative Relay Networks

3.1 Introduction

One of the main issues of current relaying networks is that the relay node has to deplete its own energy to perform such operations, which discourages idle nodes from taking part in relaying, especially when they have limited battery life. Energy harvesting (EH) relaying can resolve this issue by allowing the relay node to harvest wireless energy from an access point and to use the EH for relaying and data transmission. We name the proposed scheme in this thesis as store-then-cooperate (STC).

Generally, the wireless nodes are powered by constant battery power supply. However, replacing batteries frequency presents an inconvenient due to high number of devices. Also, this may not be possible in hazardous and remote areas where human access is limited. Impelled by the idea of wireless energy harvesting, this has received considerable research interests [33, 34]. Wireless communications links exclusively powered by ambient radio signals, such as the existing TV and radio signals, wireless information and power transfer across a noisy coupled-inductor circuit is realized in [35]. A network structure to use wireless energy transfer in hybrid cellular networks overlaid with power beacons is studied using a stochastic-geometry is presented in [36]. Wireless energy transfer was considered for cognitive radio networks in [37, 38] where secondary transmitters harvest ambient RF energy from transmissions by nearby active primary transmitters.

From [41]-[43] presents a rich literature review on the EH and contemporary overview of the state-of-the art in EH. In [45] considered a wireless-powered cooperative communication network consisting of a hybrid access point (AP). The source and the relay are depend on the energy harvested from the signals broadcast by the AP for their cooperative information transmission and authors develop harvest-then-cooperate (HTC) scheme. The physical layer network coding (PLNC) in MARS allows to improve the capacity by enabling the relay to process the received signals using xor like function and forward them to the destination [37, 39]. The relay nodes are mostly powered by limited power supply and it affects the lifetime of them. Therefore, in this thesis, we propose two main schemes using PLNC in MARS to improve the overall energy sustainability of the system. the presented approach appears to be sort of simple but effective in improving the relative system performance. This can employ in a wireless sensor networks in a remote location. In the presence of WiFi network, the proposed scheme works well as it can be used as the AP.

3.2 System model of the direct power supply scheme

The system model of the direct power supply scheme (DPS) uses QPSK signal over Rayleigh fast fading channel with additive white Gaussian noise and is based on half duplex MARS system as shown in Fig. 3.1. This system has two sources, a relay and a destination. The destination serves as an AP as well the information sink. The relay receives signals from each source and employs *Zero-forcing* detecting (ZFD) technique to detect the signal and then relay performs network coding operation on the received signals[46]. The relay retransmits the network coded signal to the destination. The destination uses network decoding operation to extract the extrinsic information received (we perform this by converting the LLRs to tanh domain) from the relay R [47] and combine with respective sources' LLRs to compute the final bit LLRs at the destination D.

The sources and relay are single input and single output (SISO) nodes with single antenna. The destination has two antennas; one for broadcasting the signal with relatively higher frequency than that of its partner antenna which is allocated for receiving the signals from other nodes.

The sources are denoted as source A and B. Both of them have direct channel links with D and also channel links through R to D. The system model consists of time cycle T with equal three time slots as shown in Fig. 3.2. Here, $\frac{T}{3}$ is the time duration allowed in each time slot.

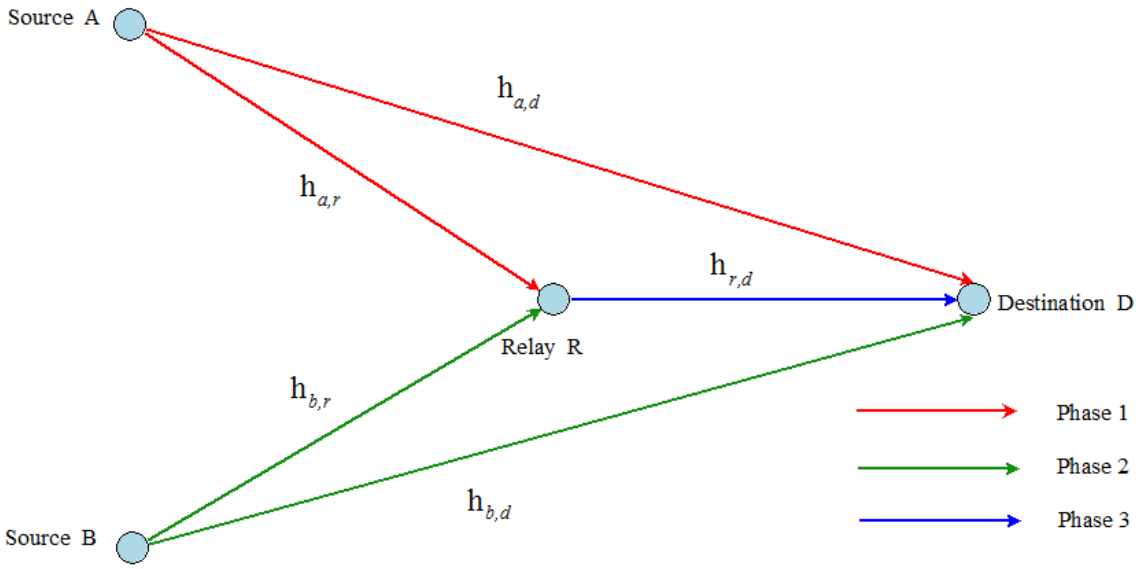

Figure 3.1: Multiple access relay channel network with DPS scheme.

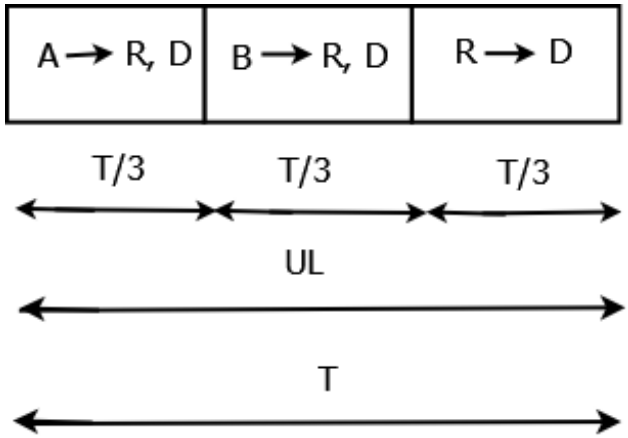

Figure 3.2: Time slot allocation diagram of DPS scheme.

We treat this conventional scheme where a direct power supply available for MARS as our baseline scheme. The following section describes all the parameters used in this chapter.

- Sources A and B are denoted as I where $I \in \{A, B\}$.
- P_I and P_R are the transmit power at the nodes I and R, respectively. X_I and X_R are QPSK signals of I and R, respectively.

- From Fig. 3.1, there are five channel links in the network. The channel link in the direction from source I to destination D is denoted as link ID. Likewise, all five channel links are represented as $\{ID, IR, RD\}$ and the distance between each node in the network is given as $\{Dist_{ID}, Dist_{IR}, Dist_{RD}\}$, respectively.
- The Rayleigh fast fading coefficients for all channel links $\{ID, IR, RD\}$ are represented as $\{H_{ID}, H_{IR}, H_{RD}\}$, respectively.
- The AWGN with zero mean and variance $N_0/2$ is the noise term which is modelled as zero mean complex Gaussian random variable. The AWGN for the links $\{ID, IR, RD\}$ are represented as $\{N_{ID}, N_{IR}, N_{RD}\}$, respectively.
- The modulo addition operation is denoted as $\oplus$.
- The extrinsic information symbol a is referred as $\widehat{a}$.
- The estimation of the information of a QPSK signal a is denominated as $\tilde{a}$.
- The log likelihood ratio (LLR) of channel links ID and RD are designated as L_{ID} and L_{RD}, respectively.

The received signals at the destination from I and R nodes in the first and second times slots, respectively, can be written as;

$$\begin{aligned} Y_{ID} &= \sqrt{P_I} H_{ID} X_I + N_{ID}, \\ Y_{IR} &= \sqrt{P_I} H_{IR} X_I + N_{IR}. \end{aligned} \tag{3.1}$$

ZFD is used to detects the real and imaginary parts of X_A and X_B from Y_{AR} and Y_{BR}, respectively at the relay.

$$\begin{aligned} &\text{if} \quad \Re(Y_{AR}) > 0 \qquad \text{then} \quad \Re(X_A) = 1; \\ &\text{if} \quad \Re(Y_{AR}) < 0 \qquad \text{then} \quad \Re(X_A) = 0; \\ &\text{if} \quad \Im(Y_{AR}) > 0 \qquad \text{then} \quad \Im(X_A) = 1; \\ &\text{if} \quad \Im(Y_{AR}) < 0 \qquad \text{then} \quad \Im(X_A) = 0; \end{aligned}$$

As in Fig. 3.1, the relay detected signals Y_{AR} and Y_{BR} are combined using network coding in the third time slot. Then, the network coded signal X_R is transmitted from R where this operation

explicates below

$$\Re(\widehat{X_R}) + j\Im(\widehat{X_R}) = X_R, \tag{3.2}$$

where $\Re(\widehat{X_R}) = \Re(\widehat{X_A}) \oplus \Re(\widehat{X_B})$, and $\Im(\widehat{X_R}) = \Im(\widehat{X_A}) \oplus \Im(\widehat{X_B})$. The received signal at D with respect to R can be written as

$$Y_{RD} = \sqrt{P_R} H_{BD} X_R + N_{RD}. \tag{3.3}$$

We use LLR as the reliability measure of the symbols at D. The LLR estimations for the real part of QPSK signals Y_{ID} and Y_{RD} are given as

$$\begin{aligned} \Re(L_{ID}) &= \frac{2\sqrt{P_I}|H_{ID}|^2}{\sigma_{ID}^2} \Re(\frac{Y_{ID}}{H_{ID}}) , \\ \Re(L_{RD}) &= \frac{2\sqrt{P_R}|H_{RD}|^2}{\sigma_{RD}^2} \Re(\frac{Y_{RD}}{H_{RD}}) . \end{aligned} \tag{3.4}$$

Similarly, we obtain the LLR estimation for imaginary part of the received symbols of Y_{ID} and Y_{RD}. The QPSK symbol X_{ID} at D is estimated by using these LLRs in (3.4). By using the diversity of the received signals at D, the extrinsic information $\widehat{L_{ID}}$ is estimated. The real and imaginary parts of extrinsic LLR of the link ID are estimated by using network decoding operation with LLR of the link[1] $\bar{I}D$ and RD as given below in $tanh$ domain

$$\tilde{L}_{ID,Real} = 2\tanh^{-1}\left\{(\tanh[\frac{\Re(L_{\bar{I}D})}{2}])(\tanh[\frac{\Re(L_{RD})}{2}])\right\} . \tag{3.5}$$

In [47], authors use (3.5) for BPSK signal and here we modified it for QPSK signal by treating QPSK symbol as two BPSK bearings. To achieve diversity, the extrinsic LLRs of X_I received from R, i.e., $\tilde{L}_{ID,Real}$, is added to bit LLRs of L_I in order to obtain $\widehat{L_I}$. We compute the real part of L_I as $\tilde{L}_{I,Real} = \tilde{L}_{ID,Real} + \Re(L_{ID})$ and similarly we obtain imaginary part. Then, we form the final LLR by combining the real and imaginary parts of L_I as

$$\tilde{L}_I = \tilde{L}_{I,Real} + j\tilde{L}_{I,Imag} . \tag{3.6}$$

The ZFD is used to map $\tilde{L}_I$ according to QPSK constellation, then, we obtain $\widehat{X_I}$ (the estimated

[1] The subscript $\bar{\text{I}}$ refers to the opposite source when source I is considered.

signal of X_I).

3.3 Energy harvesting scheme in MARS

In this chapter, we propose two energy harvesting scheme. In one the proposed schemes, radio frequency (RF) signals of AP used as a viable source for our energy harvesting scheme. In the later case, we use RF as well as stored energy in the batteries as our energy sources forming a nested energy strategies.

In this section, we discuss our first energy harvesting scheme and we denote it as EH. The energy harvesting scheme presented in this section is explained in detail in Fig. 3.5. The motivation derives for this work from [45], but we propose a simple but effective energy harvesting scheme using PLNC in MARS with battery storage scheme. Here, the destination D serves as an AP. The proposed scheme has one energy transfer phase in down link (DL) and information transfer phase – this has three time slots in uplink (UL) as in Fig. 3.3. In the energy transfer phase, D broadcasts RF signal to A, B and R. The purpose of the battery is to maintain a constant transmit power at each node as well as to store excess energy. In the following section, we present core parameters used in this chapter:

- Energy harvested in A, B and R using the transmit power P_D from destination are given as E_A, E_B and E_R, respectively.
- Energy harvesting efficiency is represented as η_{EH} where $0 < \eta_{EH} < 1$.
- Percentage of time allocated during energy transferring phase is represented as T_{EH}. Then, $T_{EH}T$ is time allocated for energy transferring phase, where $0 < T_{EH} < 1$.
- Power attenuation in the channel is given as ζ_{DI} and ζ_{DR} for channel links DI and DR, respectively.
- The time duration for information transfer phase is $\left(1 - T_{EH}T\right)$ and for each time slot is allocated $\left(\frac{(1-T_{EH})T}{3}\right)$ as shown in Fig. 3.4.

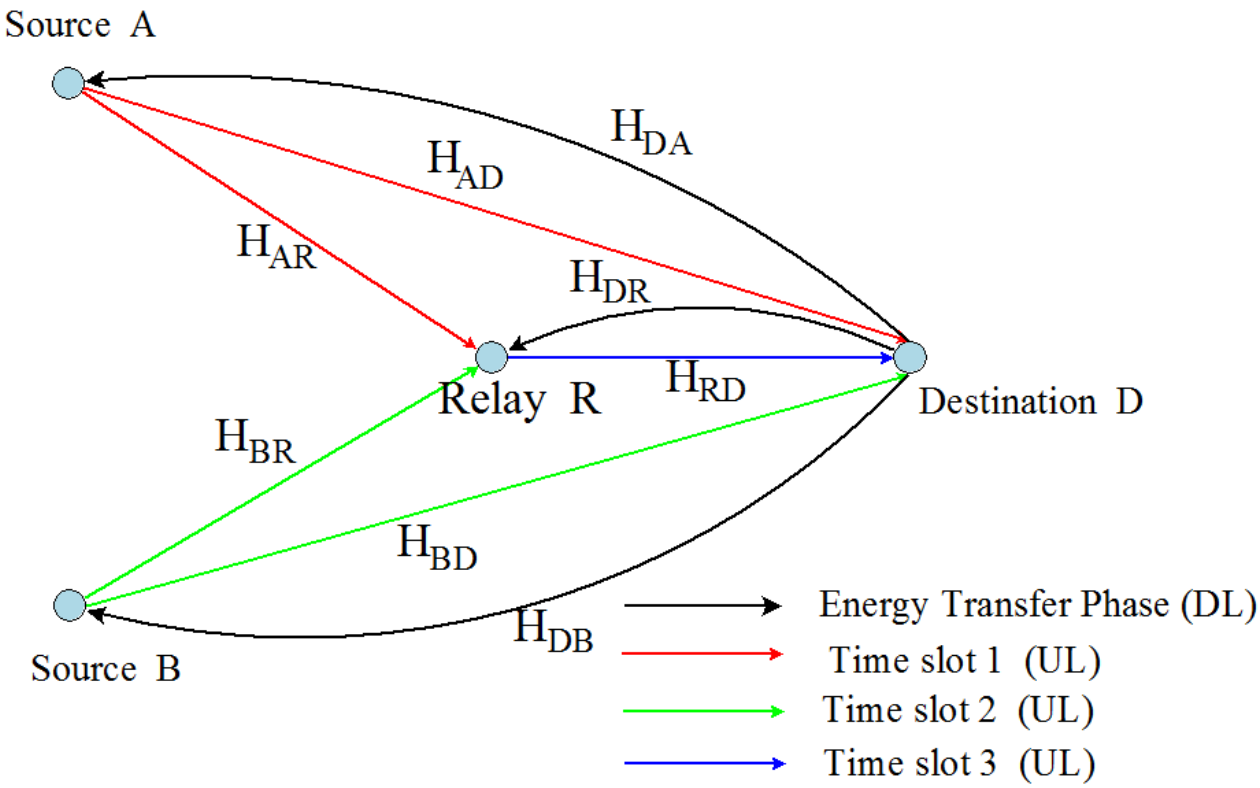

Figure 3.3: Multiple access relay channel network with energy harvesting scheme.

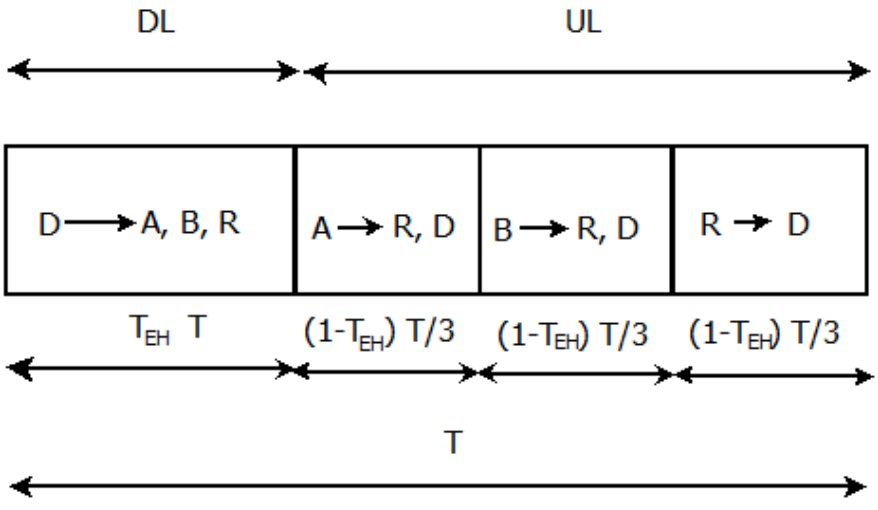

Figure 3.4: Time slot allocation diagram of energy harvesting scheme of the MARS.

E_I and E_R are computed as

$$E_I = \eta_{EH}(T_{EH}T)P_D\zeta_{DI}\,,$$
$$E_R = \eta_{EH}(T_{EH}T)P_D\zeta_{DR}\,. \tag{3.7}$$

As the harvested energy in all the nodes are variable in nature, the amount of power drawn from

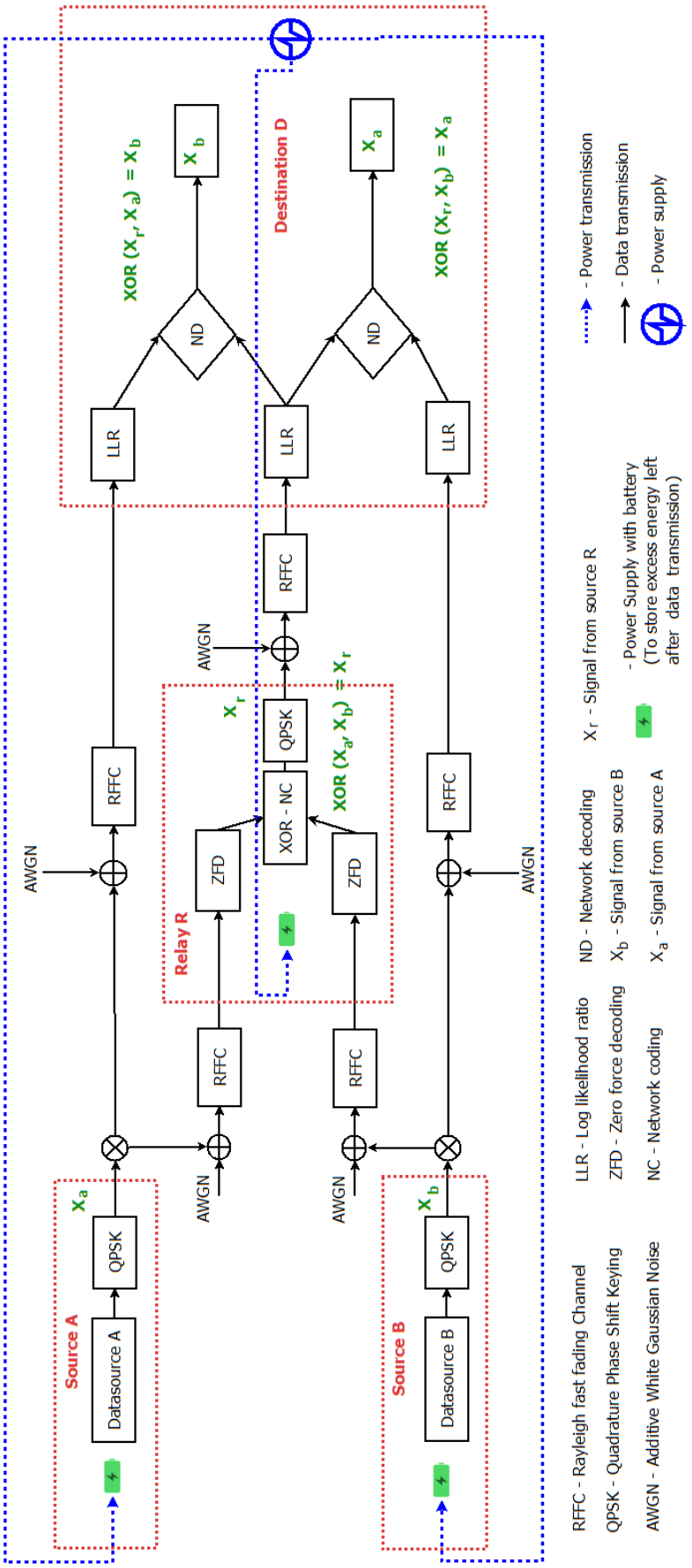

Figure 3.5: The proposed system model with energy harvesting scheme.

these nodes may not be equal to the power constrain set in our base-line DPS scheme. Further, each node may harvest different amount of energy from the RF signal. Therefore, we maintain constant transmit power by storing excessive energy in each battery and by consuming only the required threshold energy at each node per time cycle. The variable $E_{Th,EH}$ is the threshold energy needed to maintain a constant transmit power at each node. The energy in excess of $E_{Th,EH}$ is stored in a Lithium-ion battery, where the efficiency of battery is denoted as η_{Bt} [49]. This excess energy stored in the batteries provides a base for our next propose scheme. We set the signal transmit power for node I and R in EH to be P_{node} which is approximately equal to the power transmit of node I and R in the base-line DPS scheme.

$$P_I = P_R = P_{node}\,. \tag{3.8}$$

Threshold energy $E_{Th,EH}$ is calculated using P_{node} as

$$E_{Th,EH} = (P_{node}(1 - T_{EH})\,T)/3\,. \tag{3.9}$$

The batteries in I and R are represented as Bt_I and Bt_R, respectively. The energy saved in the battery Bt_I and Bt_R are denoted as $E_{I,S}$ and $E_{R,S}$, respectively.

$$\begin{aligned} E^{+}_{R,S} &= E_{R,S} + (E_R - E_{Th,EH})\eta_{Bt}\,, \\ E^{+}_{I,S} &= E_{I,S} + (E_I - E_{Th,EH})\eta_{Bt}\,, \end{aligned} \tag{3.10}$$

where, $E^{+}_{R,S}$ and $E^{+}_{I,S}$ denotes the current state of energy level in battery Bt_R and Bt_I, respectively, this energy is used as our base energy in the next proposed scheme, i.e. *store-then-cooperate* scheme. $E_{R,S}$ and $E_{I,S}$ denotes the previous state of energy level in battery Bt_R and Bt_I, respectively. Battery Bt_R will charge rapidly as compared to Bt_I because energy harvested in R is higher than that of I due to shorter distance as compared to I. From (3.7), the impact of distance on power attenuation is elucidated. This follows that the distance d is inversely proportional to harvested energy E as shown below

$$d \propto \frac{1}{E} \tag{3.11}$$

We set the energy storage limit of Bt_R to $E_{R,limit}$. When the energy level $Bt_R \geq E_{R,limit}$, a pilot message is sent to all the nodes from R, then our system switches from EH scheme to the new energy harvesting scheme called *store-then-cooperate*.

3.4 Store-then-cooperate scheme in MARS

In this section, we propose a new scheme called *store-then-cooperate* (STC) and that is complementary to EH scheme. The model is shown in Fig. 3.6 and used to harvest energy without affecting the information transfer phase. In this STC scheme, our information transfer phase and energy harvesting phase are divided into three equal counterparts as in Fig. 3.7. The energy transfer phase is coincide with the information transfer phase limited by the time slot duration $\frac{T}{3}$ and allowing a significant increment in throughput as compared to its partner scheme of EH. The Energy harvesting in each node happens when the node is not involved in information transmission or receiving at any given time slot. Each source has two energy harvesting time slots; each source harvests energy separately in time slots one and two, respectively, while both the sources harvest energy at the third time slot simultaneously. The relay does not harvest energy in STC scheme at R. Therefore, the energy stored in the battery will be used as there is no energy harvesting or power supply is available in STC. The amount of time allocated for information processing equal in both STC and DPS schemes.

The energy stored in the battery at each node in EH is used as the energy resource for the MARS in STC. The EH has two distinctive features that can be complemented by this new scheme;

- The energy harvested in relay will be higher than the energy harvested in sources because the distance between the relay and destination is shorter than distance between sources and destination.
- EH has separate phases for the energy harvesting and information transfer.

The STC complements the EH by

- One of the advantages of this scheme is that it does not have to allocate a separate time slot for energy harvesting and information transfer. Both energy transfer and information

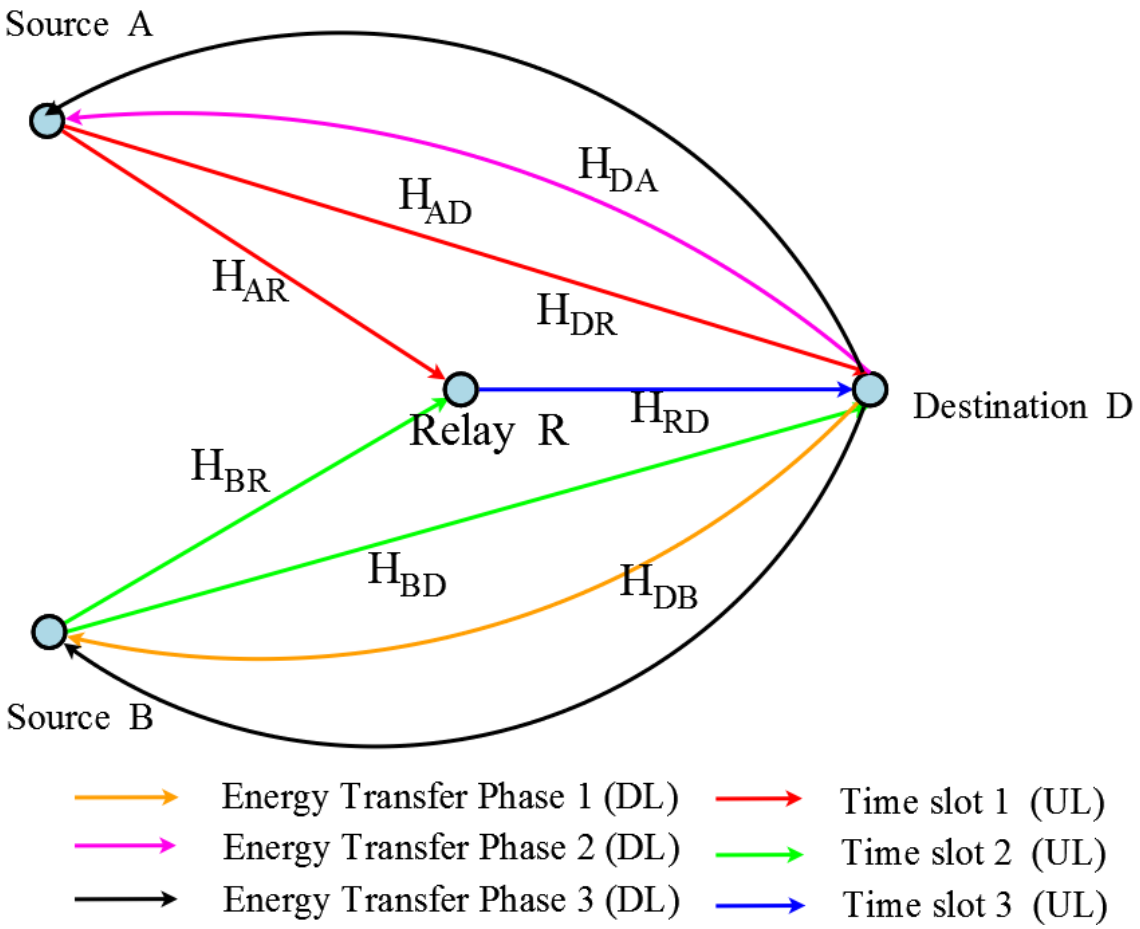

Figure 3.6: MARS with store-then-cooperate scheme. Sources *A* and *B* harvests energy from the destination *D*.

transfer happens simultaneously at different nodes.

- In the STC, only the sources harvests energy from the signal transmitted by the destination. The relay can not harvest energy because it receives data from sources in time slot one and two and transmits data to the destination in the third time slot.
- The proposed STC scheme does not require energy supply from any external resource as in EH scheme. However, STC sustain and make fully exploitation of the energy harvested in EH scheme while improving the throughput.

Since both schemes complementing each other to maintain a balance in energy harvesting and storage, we propose a dynamic switch between two schemes in a cyclic process to maintain constant energy supply to the system to maintain the target SER.

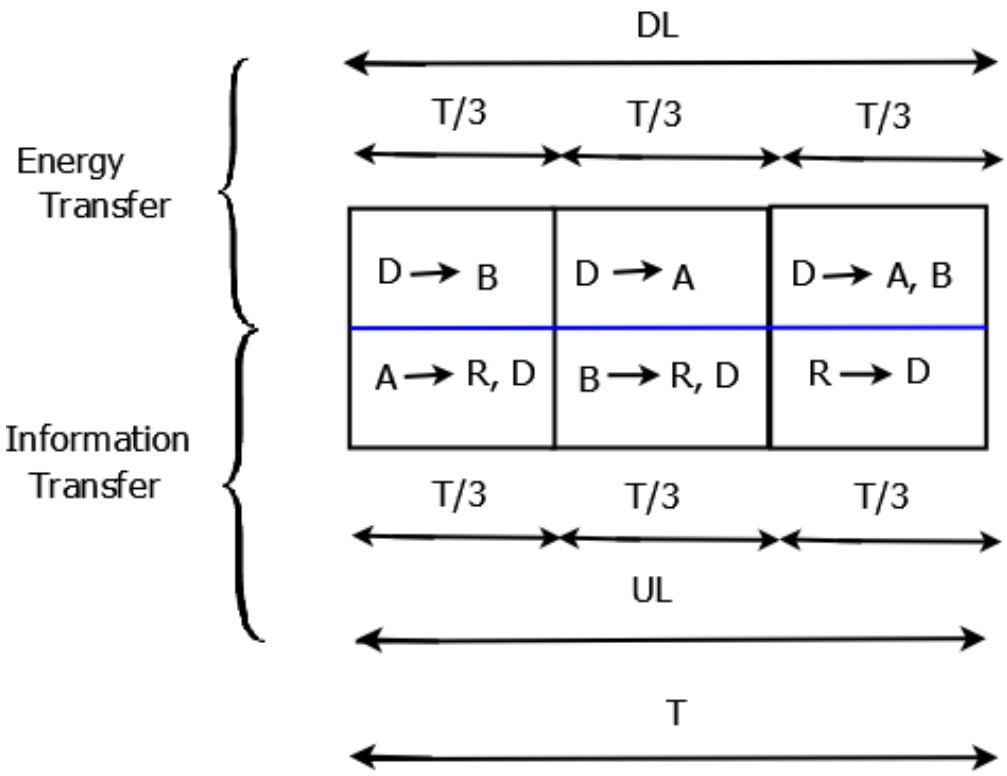

Figure 3.7: Time allocation diagram of store-then-cooperate scheme.

Our proposed STC scheme harvests energy twice at each source node in two different time slots for a time duration $\frac{T}{3}$ as shown in Fig. 3.7. Then, the energy harvested at each node, $E_{I,STC}$, can be written as

$$E_{I,STC} = 2\eta_{EH}\frac{T}{3}P_D\zeta_{DI}\,. \tag{3.12}$$

We use a new energy threshold to maintain the same transmit power as in MARS with DPS scheme and MARS with EH. The threshold energy is varied depending on time allocation for harvesting and transmitting information. Threshold energy in STC is denoted as $E_{Th,STC}$ and computed using P_{node}.

$$E_{Th,STC} = (P_{node}T)/3\,. \tag{3.13}$$

This $E_{Th,STC}$ is used for the generating signal transmit power in STC scheme.

At each node, $E_{Th,STC}$ and $E_{Th,EH}$ are energy thresholds in the STC and EH to keep the signal transmitting power equal and constant as our base-line DPS scheme. As the relay is completely depend on the Bt_R for energy demand, in STC, the energy stored in Bt_R will gradually reduce

in every time cycle. If $E_{I,STC}$ is less than $E_{Th,STC}$, then, energy is utilized from Bt_I, otherwise excessive energy will be stored in Bt_I as

$$E^{+}_{I,S} = E_{I,S} + (E_{I,STC} - E_{Th,STC})\eta_{Bt}\,. \tag{3.14}$$

When the relay utilizes its stored energy, $E_{R,S}$, for signal transmission, we have

$$E^{+}_{R,S} = E_{R,S} - (E_{Th,STC}/\eta_{Bt})\,. \tag{3.15}$$

Here, $E^{+}_{R,S}$ and $E^{+}_{I,S}$ denotes the current state of energy level in battery Bt_R and Bt_I, respectively. $E_{R,S}$ and $E_{I,S}$ denotes the previous state of energy level in battery Bt_R and Bt_I, respectively in STC. When $E_{R,S}$ in Bt_R drops below twice the value of $E_{Th,STC}$ then, a pilot message is sent to all the nodes from R then the system switches from STC to EH. Next, we present the dynamic switch formed by these nested energy strategies, i.e., EH and STC.

Data: Algorithm for dynamic switch
while *True* **do**
  EH scheme
  if $(E_{R,S,\zeta_1} \leq E_{R,limit})$ **then**
    $E_{R,S,\zeta_1} = E_{R,S,(\zeta_1-1)} + E_{Th,STC}\eta_{Bt}$, for $\zeta_1 = 1,..,\mathbb{T}_1$;
  else
    MARS switches to STC
    if $(E_{R,S,\zeta_2} \geq 2E_{Th,STC})$ **then**
      $E_{R,S,\zeta_2} = E_{R,S,(\zeta_2-1)} - E_{Th,STC}/\eta_{Bt}$, for $\zeta_2 = 2,..,\mathbb{T}_2$;
    end
  end
end

Algorithm 1: The proposed dynamic switch of EH and STC schemes

Where $\mathbb{T}_1$ and $\mathbb{T}_2$ represents the total time cycles that EH and STC undergo until this satisfies the energy constraint as determined in this algorithm.

3.5 Outage probability analysis of MARS

In this section, the outage probability of DPS scheme is studied. The target rate is expressed as $\frac{3k}{2}$, where k is the data rate per block per second. The outage probability of the system is considered in the following two scenarios:

Criteria OP1: The successful delivery with achievable full diversity if

1. Both signals X_A and X_B are delivered to the destination.
2. Both signals X_A and X_B achieve full diversity at the destination by successful signal transmission from their respective source link and the relay link.

Criteria OP2: The successful delivery if

1. Both signals X_A and X_B are delivered to the destination.

A failure and success events of channel link ID to transmit a signal is represented as $P(\overline{ID})$ and $P(ID)$, respectively. Outage probability of MARS is estimated using the signal to noise ratio (SNR) of each channel link in the MARS. SNR of link ID is given as $\Gamma_{ID} = \frac{P_A|H_{ID}|^2}{N_0}$. Therefore, probability of channel link ID can be estimated as fallows:

$$\begin{aligned} P(\overline{ID}) &= P\Big(\Gamma_{ID} < 2^{(3/2)k} - 1\Big) = 1 - \mathrm{EXP}\bigg(-\frac{2^{(3/2)k}-1}{\Gamma_{ID}}\bigg), \\ P(ID) &= P\Big(\Gamma_{ID} > 2^{(3/2)k} - 1\Big) = \mathrm{EXP}\bigg(-\frac{2^{(3/2)k}-1}{\Gamma_{ID}}\bigg). \end{aligned} \tag{3.16}$$

Similarly, the outage probability for all the individual channel links $\{ID, RD\}$ can be defined as in (3.16). The probability of event receives a signal is estimated at two receiving nodes of R and D. At the relay, if the signals from both the sources are received successfully then it is a success event otherwise a failure. This failure event is represented as $P(\overline{E_R})$ and successful event is represented as $P(E_R)$. The following equation satisfies for both $OP1$ and $OP2$ for receiving node R;

$$\begin{aligned} P(E_R) &= P(AR)P(BR)\,, \\ P(\overline{E_R}) &= 1 - P(E_R)\,. \end{aligned} \tag{3.17}$$

The probability of failure and success events occurring at D with respect to the criteria $OP1$ considering that the event $P(E_R)$ occurs at relay. Failure event denotes as $P(\overline{E_{D,OP1}})$ and successful event represents as $P(E_{D,OP1})$, now we have

$$\begin{aligned} P(E_{D,OP1}) &= P(AD)P(BD)P(RD)\,, \\ P(\overline{E_{D,OP1}}) &= 1 - P(E_{D,OP1})\,. \end{aligned} \tag{3.18}$$

Probability of failure event $P(\overline{\text{MARS-OP1}})$ of the system with respect to $OP1$ is given by

$$P(\overline{\text{MARS-OP1}}) = P(\overline{E_R}) + \quad P(E_R)P(\overline{E_{D,OP1}})\,. \tag{3.19}$$

Probability of failure event of the system with respect to $OP2$ denotes as $P(\overline{\text{MARS-OP2}})$ and is computed by.

$$\begin{aligned} P(\overline{\text{MARS-OP2}}) = {} & P(\overline{AD})P(\overline{BD}) + P(\overline{AD})P(BD)P(E_R)P(\overline{RD}) \\ & + P(\overline{AD})P(BD)P(\overline{E_R}) + P(AD)P(\overline{BD})P(E_R)P(\overline{RD}) \\ & + P(AD)P(\overline{BD})P(\overline{E_R}) \end{aligned} \tag{3.20}$$

3.6 Outage probability analysis of MARS with EH and STC

In outage probability analysis of MARS with energy harvesting scheme, the energy transfer and information transfer phases need to be considered for outage events. In Section 3.5, both the sources and relay obtain reliable power supply and therefore outage happens only due to link failures. The units of energy and power defined as $Joules$ and $Watts$, respectively. Based on this system model and Fig. 3.4, the time allocated for information transfer in DPS scheme is T and for EH is $(1 - T_{EH})T$. The target rate is expressed as $\frac{3k}{2}$ where k is the data rate per block per second for DPS scheme. In case of EH as in Fig. 3.4, the target rate is taken as $\frac{3k}{2}\left(\frac{1}{(1-T_{EH})}\right)$. This clearly shows that more data needs to be sent in EH per time frame than that of non-energy harvesting scheme such as DPS. Outage occurrence due to energy transfer is dealt in EH by transmitting a justifiable power. The outage probability of information transfer is increased in

EH as compared to MARS with DPS scheme. The equation (3.16) can be modified as

$$P(\overline{ID}) = P\left(\Gamma_{ID} < 2^{\frac{3k}{2}\left(\frac{1}{(1-T_{EH})}\right)} - 1\right) = 1 - \text{EXP}\left(-\frac{2^{\frac{3k}{2}\left(\frac{1}{(1-T_{EH})}\right)} - 1}{\Gamma_{ID}}\right)$$
$$P(ID) = P\left(\Gamma_{ID} > 2^{\frac{3k}{2}\left(\frac{1}{(1-T_{EH})}\right)} - 1\right) = \text{EXP}\left(-\frac{2^{\frac{3k}{2}\left(\frac{1}{(1-T_{EH})}\right)} - 1}{\Gamma_{ID}}\right) \tag{3.21}$$

substituting (3.21) in (3.19) gives outage probability of EH for successful information transfer with maximum achievable diversity as in criteria $OP1$ is for $P(\overline{\text{MARS-OP1}_{EH}})$. Moreover, substituting (3.21) in (3.20) gives the outage probability of EH for successful information transfer as in criteria $OP2$ is for $P(\overline{\text{MARS-OP2}_{EH}})$.

The outage probability of STC is equal to that of DPS scheme because the time duration for the information transfer and the signal transmit power are equal due to the simultaneous energy and information transfer in STC. It is not sacrifice time slot resources for energy transfer as in EH scheme.

3.7 Numerical results

In this section, we discuss the simulation setup and demonstrate the performance of the proposed energy harvesting schemes. The distance between nodes are assumed as $Dist_{AD} = Dist_{BD} = 20m, Dist_{BR} = Dist_{AR} = 18m, Dist_{RD} = 2m$ with the path loss exponent for free space, $\Psi = 2$ and signal power attenuation of 30dB per meter [48]. The number of symbols is 10^6 which is transmitted through the in Rayleigh fast fading and AWGN channels. The total transmit power is $P_d = 30$ dbm in DPS scheme and $P_d = 83.9794$ dBm in EH and STC schemes. The SNR ranges between 0 to 36 dB and the data rate $k = 0.5$. The energy harvesting efficiency is 50%[43] and we set $T = 1$. The time allocated from each time cycle for energy transferring phase, T_{EH} is 30%. Lithium-ion battery has a charging and discharging efficiency of $\eta_{Bt} = 0.9$ as in [49]. Predefined threshold limit of battery at relay $E_{r,Limit} = 20\ Joules$ i.e. 0.0055555556 $watt-hour$. Fig. 3.8 shows the symbol error rate (SER) performance of DPS, EH and STC schemes. This figure demonstrates successful maintenance of target SER of MARS approximately at equal level

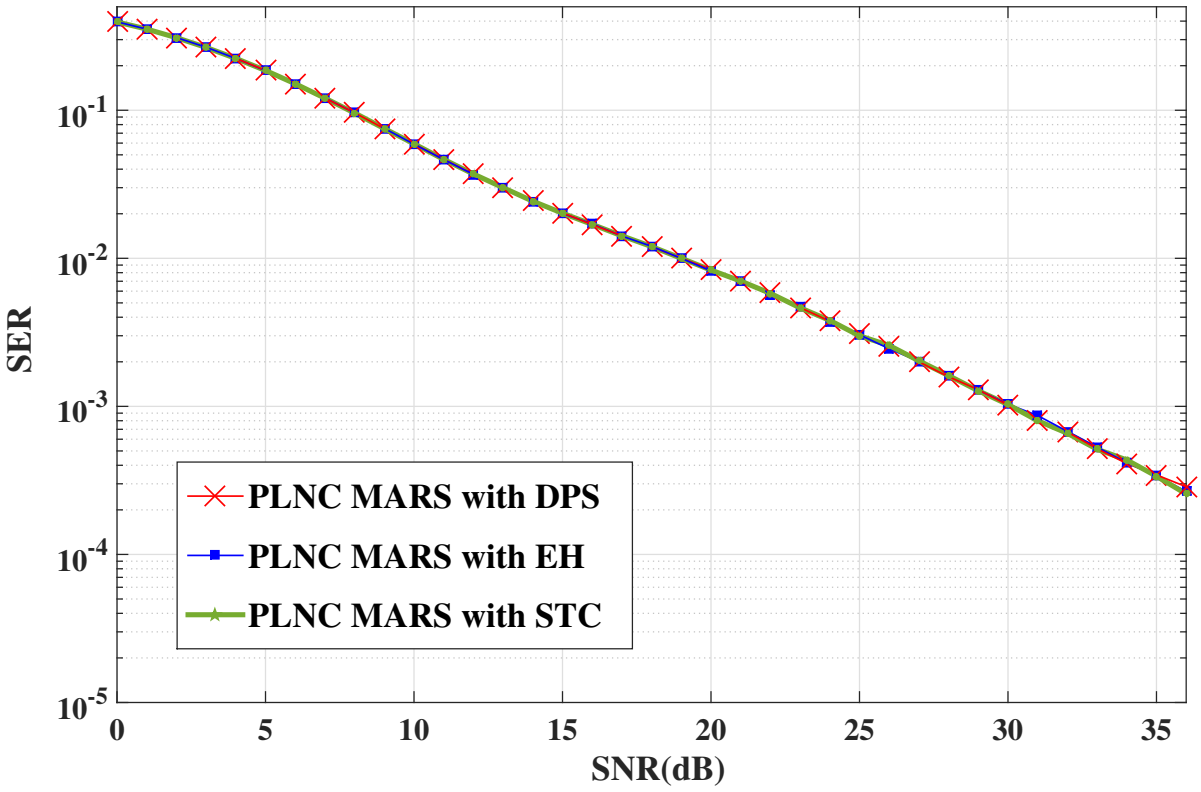

Figure 3.8: Comparison of SER MARS with PLNC with DPS scheme, EH and STC over Rayleigh fast fading with AWGN channels. The distances $Dist_{AD} = Dist_{BD} = 20m, Dist_{BR} = Dist_{AR} = 18m, Dist_{RD} = 2m$.

in all the three schemes for respective SNR levels. Consistency of SER level is due to maintaining equal and constant signal transmit power in both the sources and relay in EH and STC by carefully adjusting the time allocation between the energy harvesting and information transfer where appropriate.

Fig. 3.9 shows comparison of outage probability of MARS with DPS, EH and STC scheme for criteria $OP1$ and $OP2$. In general, criteria $OP1$ will have higher outage probability than that of criteria $OP2$. The outage probability of EH is higher than the DPS and STC because of the time available for information transfer in EH is lessen as compared to other two competitive schemes. The outage probability of both STC and DPS scheme are in same parity due to equal time allocation for information transfer phase.

Fig. 3.10 demonstrates the battery charging rate is higher at relay than at source. Energy stored

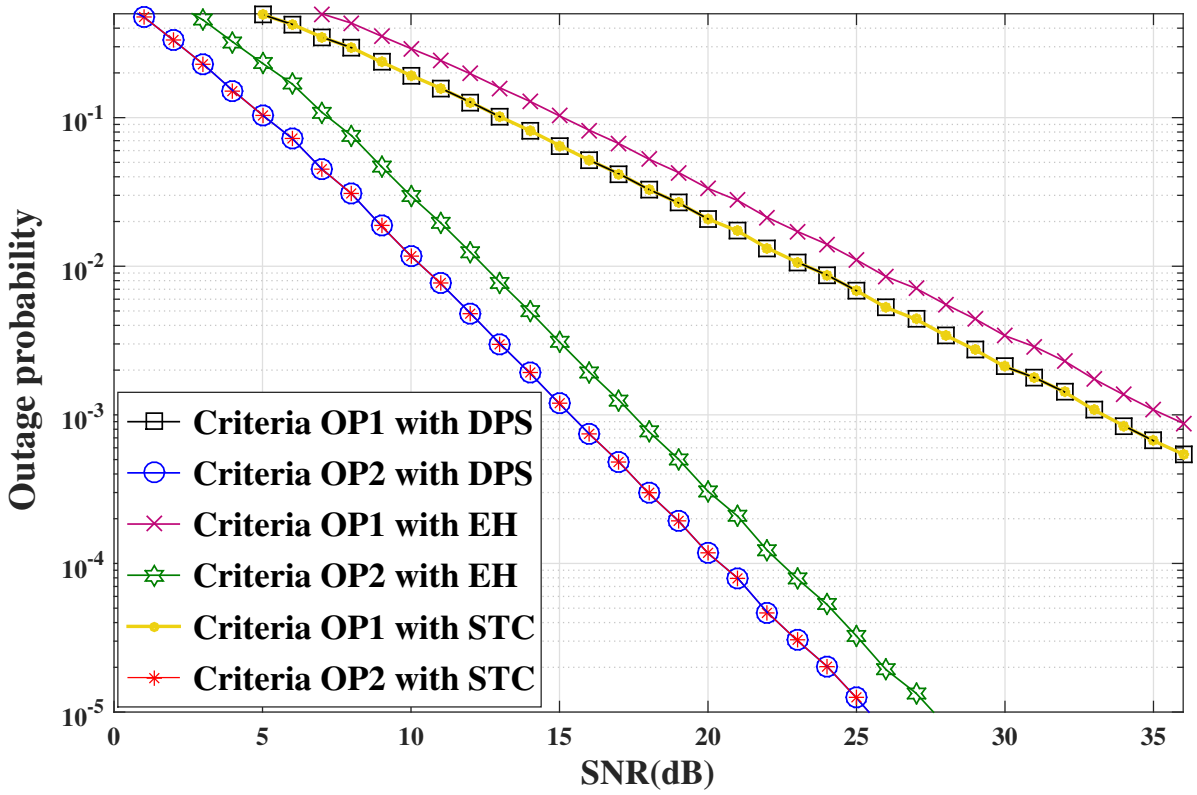

Figure 3.9: Comparison of outage probability for MARS with different criteria and energy harvesting scheme. The curves in the graphs are the result of equations (3.19) $P(\overline{\text{MARS-OP1}})$, (3.20) $P(\overline{\text{MARS-OP2}})$, Section 3.6 $P(\overline{\text{MARS-OP1}_{EH}})$ and Section 3.6 $P(\overline{\text{MARS-OP2}_{EH}})$. The distances $Dist_{AD} = Dist_{BD} = 20m, Dist_{BR} = Dist_{AR} = 18m, Dist_{RD} = 2m$.

in the battery depends on the harvested energy. The difference in harvested energy is due to relative higher gain in relay to destination channel as compared to the gain from source to destination channel. The channel gain decreases with distance between nodes due to path loss factor. The relationship between the distance, path loss exponent and power attenuation of broadcasting signal for channel AD can be represented as $Dist_{AD}^{-\Psi} \times 10^{-3}$. It is evident from this figure by comparing batteries Bt_A and Bt_B as they have similar in charging rate. For this simulation setup Bt_R takes 16 time cycles to charge up to 21.59 $Joules$ i.e., 0.005997 $watt-hour$. When Bt_R reaches above 0.0055555556 $watt-hour$, EH switches to STC.

Fig. 3.11 demonstrates gradual decrease in energy with each time cycle in Bt_R because the relay uses energy stored in Bt_R for signal transmission. The energy in batteries Bt_A and Bt_B increase at constant rate with time due to energy harvesting in sources as in Fig. 3.6. The STC

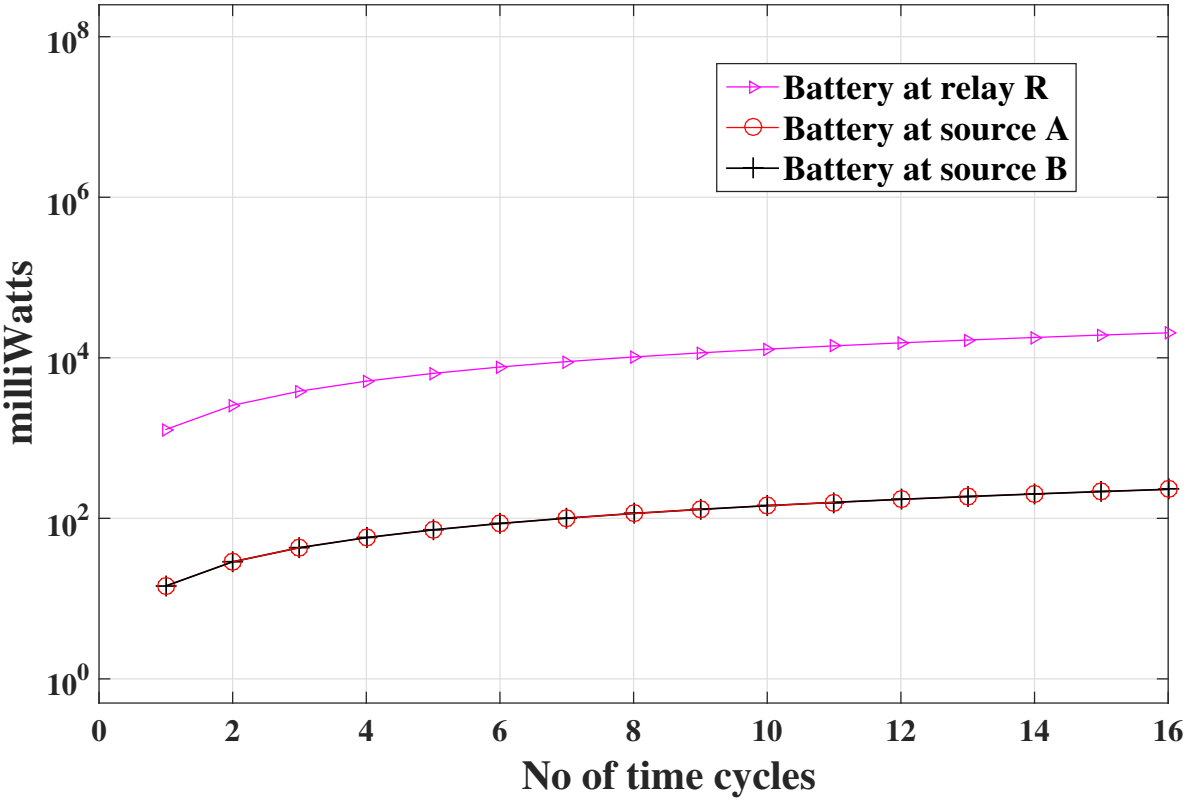

Figure 3.10: Comparison of batteries charging at the sources and the relay for each time cycle of the MARS with EH. The distances $Dist_{AD} = Dist_{BD} = 20m, Dist_{BR} = Dist_{AR} = 18m, Dist_{RD} = 2m$.

scheme continues until the energy reaches below twice the value of $E_{Th,STC}$ i.e. twice the value of 111.11 $milliJoules$ in Bt_R. It uses 21.59 $Joules$ to sustain upto 165 time cycles to reach 111.11 $milliJoules$. This is the energy as a available backup power source for relay for 2 time cycles.

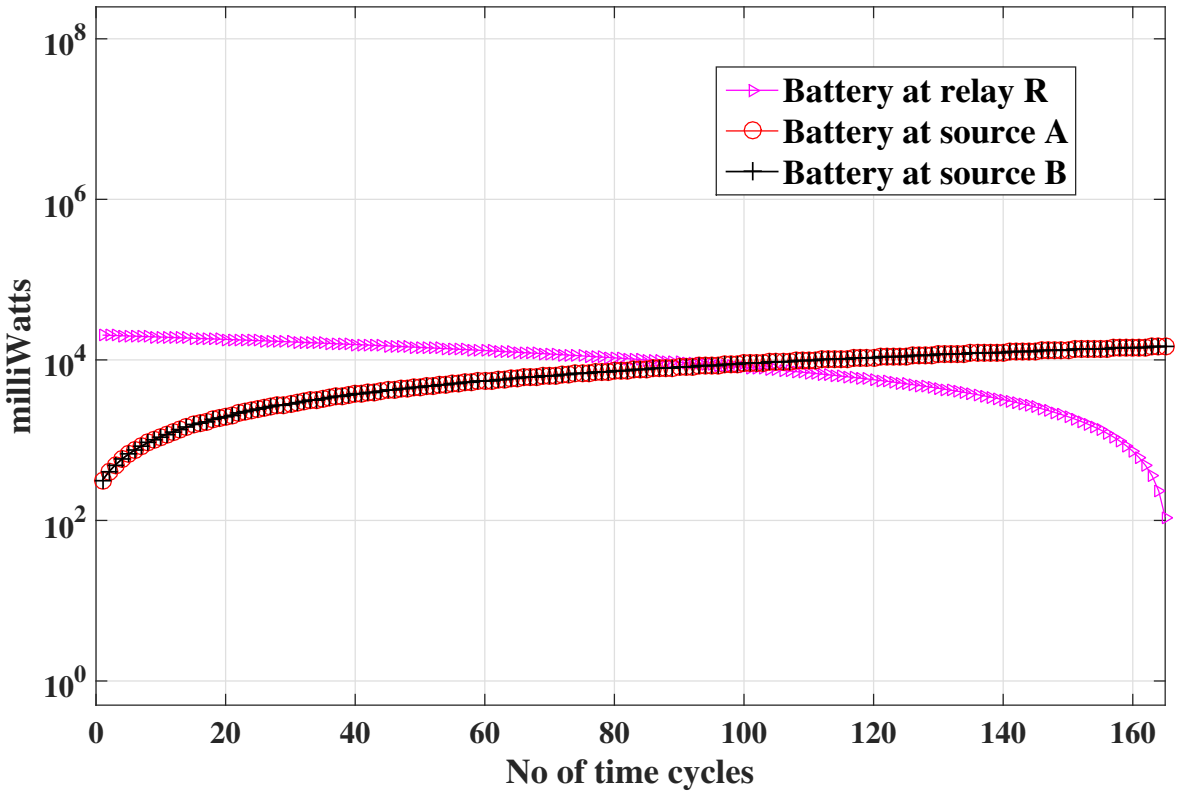

Figure 3.11: Utilization of stored power from the battery at relay and charging of batteries in other nodes in MARS with STC. The distances $Dist_{AD} = Dist_{BD} = 20m, Dist_{BR} = Dist_{AR} = 18m, Dist_{RD} = 2m$.

4. Conclusions and Future Work

4.1 Conclusions

With the analysis of parallel relay network using AF protocol, as in Table 2.1 and Fig. 2.6, we study the ratio of the rate of improvement in channel gain with respect to the increase in a number of relays. This ratio can help in estimating the advantages and disadvantages of adding more relays to the existing system in order to combat multipath propagation. It is advantageous to add a relay to the system if the improvement in the system performance is significant enough. Thereby we can find a break even between the number of relays added to the network and its relative contribution to the performance.

Two different energy harvesting schemes for MARS are successfully implemented together with a direct power supply scheme. By using batteries in each node, we store excessive energy. This approach forms a core of a newly proposed scheme, called store-then-cooperate. Two different frequencies are used for data and energy transfer, thus avoiding the need for time division between these two tasks. The symbol error rate achieved in this new scheme is similar to that of the scheme with a direct power supply. We study impact of energy harvesting schemes on the outage probability of the system and observe that time allocation for the information transfer and energy harvesting affects the outage probability. The introduction of STC allows the system to improve its performance by reducing the outage probability, and the resulting performance is comparable to that of the DPS scheme. From the analysis in Section 3.4, we observe that EH and STC complements each other by creating a balance in energy harvesting. We also introduce a dynamic switch between EH and STC schemes in order to maintain the balance between the

amount of harvested energy in the relay and in the sources. The proposed schemes can be used near high power wifi routers in order to harvest energy.

4.2 Future work

- Implementation of energy harvesting scheme together with information transmission in the parallel relay network by optimizing the power utilization in all the nodes in the network for improving the performance of cooperative communication.
- A comparative study for the best diversity combining strategy in the destination.
- Simultaneous wireless information and power transfer used for the proposed STC scheme in a full duplex system.
- In our EH and STC scheme, we kept constant signal transmitting power to maintain SER at same level. However, it may be possible to use an efficient there can be estimation for optimum signal transmitting power to maintain SER a same level without affecting outage probability of system.
- Implementing our scheme with powerful channel codes like low-density-parity-codes can be a promising way to improve coding gain.

Bibliography

[1] C. E. Shannon and W. Weaver, "The Mathematical Theory of Communication," *University of Illinois Press*, 1949.

[2] D. Tse and P. Viswanath, "Fundamentals of wireless communication," *Cambridge University Press*, 2005.

[3] J. N. Laneman and G. W. Wornell, "Distributed space-time coded protocols for exploiting cooperative diversity in wireless networks," *IEEE Trans. Info. Theory*, vol. 40, no. 10, pp. 2415–2425, Oct. 2003.

[4] T. M. Cover and A. El Gamal, "Capacity theorems for the relay channel," *IEEE Trans. Info. Theory*, vol. 25, no. 5, pp. 572-584, Sept. 1979.

[5] E. Van der Meulen, "A survey of multi-way channels in information theory: 1961-1976," *IEEE Transactions on Information Theory*, vol. 23, no.1, pp. 1–37, 1977.

[6] A. Sendonaris, E. Erkip, and B. Aazhang, "User cooperation diversity-Part I: System description," *IEEE Trans. on Information Theory*, vol. 51, no. 7, pp. 1927–1938, November 2003

[7] A. Sendonaris, E. Erkip, and B. Aazhang, "User cooperation diversity-Part II: Implementation aspects and performance analysis," *IEEE Trans. on Information Theory*, vol. 51, no. 7, pp. 1939–1948, November 2003

[8] A. Nosratinia, T. E. Hunter, and A. Hedayat. "Cooperative communication in wireless networks", *IEEE Communications Magazine*, vol.42, no.10, pp. 74–80, Oct. 2004.

[9] T.E. Hunter and A. Nosratinia, "Cooperative communication in wireless networks", *IEEE Trans. on Wireless Communication*, vol. 5, no. 2, pp. 283–289, Feb. 2006.

[10] Z. Zhang, "Partial converse for a relay channel", *IEEE Trans. Info. Theory*, vol. 34, no. 5, pp. 1106-1110, Sept. 1988.

[11] C.M. Zeng, F. Kuhlmann and A. Buzo, "Achievability proof of some multiuser channel coding theorems using backward decoding", *IEEE Trans. Info. Theory*, vol. 35, no. 6, pp. 1106-1165, 1989.

[12] J. A Thomas, "Feedback can at most double Gaussian multiple access channel capacity", *IEEE Trans. Info. Theory*, vol. 35, no. 6, pp. 711–716, 1987.

[13] R.C. Hill, W. E. Griffiths, and G. C. Lim, "Principles of econometrics", vol. 5. *Hoboken, NJ: Wiley*, 2008.

[14] J. Neyman and E. S. Pearson, "On the problem of the most efficient tests of statistical hypotheses", *Philosophical Transactions of the Royal Society A: Mathematical, Physical and Engineering Sciences* , vol. 231, pp. 289-337, 1933.

[15] S. Zhang, S. C. Liew and P. P. Lam, “Hot topic: physical-layer network coding,” *ACM Mobicom.*, pp. 358–365, 2006.

[16] L. Xiao, T. Fuja, J. Kliewer, and D. Costello. "A network coding approach to cooperative diversity", *IEEE Trans. Inf. Theory*, vol. 53, no.10, pp. 3714–3722, Oct. 2007.

[17] H. Visser and R. Vullers, "RF energy harvesting and transport for wireless sensor network applications: Principles and requirements," *Proceedings of the IEEE*, vol. 101, no. 6, pp. 1410–1423, June 2013.

[18] X. Lu, P. Wang, D. Niyato, and Z. Han, "Resource allocation in wireless networks with rf energy harvesting and transfer," *IEEE Communications Surveys and Tutorials*, 2014.

[19] X. Lu, P. Wang, D. Niyato, D. I. Kim, and Z. Han, "Wireless networks with RF energy harvesting: A contemporary survey," available online: http://arxiv.org/abs/1406.6470, 2014.

[20] V. Liu, A. Parks, V. Talla, S. Gollakota, D. Wetherall, and J. R. Smith, "Ambient backscatter: Wireless communication out of thin air," *Proceedings of the ACM SIGCOMM* , 2013.

[21] S.C. Liew, S. Zhang and L. Lu, "Physical-Layer Network Coding: Tutorial, Survey, and Beyond," *Physical Communication*, 2013.

[22] S. Kim, R. Vyas, J. Bito, K. Niotaki, A. Collado, A. Georgiadis, and M. M. Tentzeris, "Ambient RF energy-harvesting technologies for self sustainable standalone wireless sensor platforms," *Proc. IEEE*, vol. 102, no. 11, pp. 1649-1666, Nov. 2014

[23] I. Flint, X. Lu, N. Privault, D. Niyato, and P. Wang, " Performance analysis of ambient RF energy harvesting: a stochastic geometry approach," *Proc. IEEE Glob. Commun. Conf.*, pp. 1448-1453, 2014.

[24] K. Huang and X. Zhou, "Cutting the last wires for mobile communications by microwave power transfer," *IEEE Commun. Mag.*, vol. 53, no. 6, pp. 86-93, Jun. 2015.

[25] S. He, J. Chen, F. Jiang, D. K. Y. Yau, G. Xing, and Y. Sun, "Energy provisioning in wireless rechargeable sensor networks," *IEEE Trans. Mobile Comput.*, vol. 12, no. 10, pp. 1931-1942, Oct. 2013.

[26] J. N. Laneman, D. Tse and G. W. Wornell, "Cooperative diversity in wireless networks: Efficient protocols and outage behavior," *IEEE Trans. Info. Theory*, vol. 50, no. 12, pp. 3062–3080, Dec. 2004.

[27] T. M. Cover and A. El Gamal, "Capacity theorems for the relay channel," *IEEE Trans. Info. Theory*, vol. 25, no. 5, pp. 572–584, Sept. 1979.

[28] G. Kramer, M. Gastpar, and P. Gupta, "Cooperative strategies and capacity theorem for relay networks," *IEEE Trans. Info. Theory*, vol. 51, no. 9, pp. 572–584, Sept. 2005.

[29] I. Maric and R. D. Yates, "Forwarding strategies for Gaussian parallel-relay networks," *IEEE International Symposium on Information Theory (ISIT)*, pp. 269, Sept. 2004.

[30] J. G. Proakis, "Digital Communications," *4th ed., New York: McGraw-Hill*, 2001.

[31] K. J. R. Liu, A. K. Sadek, W. Su, A. Kwasinski, "Cooperative Communications and Networking," *Cambridge University Press, New York*, 2008.

[32] J. Laneman, D. Tse, G. Wornell, "Cooperative Diversity in Wireless Networks: Efficient Protocols and Outage Behavior," *IEEE Trans. Inf. Theory*, vol. 50, no. 12, pp. 3062–3080, Dec. 2004.

[33] B. Medepally and N. B. Mehta, " voluntary energy harvesting relays and selection in cooperative wireless networks," *IEEE Trans. Wireless Commun.*, vol. 9, no. 11, pp. 3543–3553, Nov. 2010.

[34] W. Lumpkins, " Nikola Tesla's dream realized: Wireless power energy harvesting," *IEEE Consumer Electron. Mag.*, vol. 3, no. 1, pp. 39–42, Jan. 2014.

[35] P. Grover and A. Sahai, "Shannon meets Tesla: Wireless information and power transfer," *in Proc. 2010 IEEE Int. Symp. Inf. Theory* , pp. 2363–2367, Austin, USA, Jun. 2010.

[36] K. Huang and V. Lau, "Enabling wireless power transfer in cellular networks: Architecture, modeling and deployment,"*IEEE Trans. Wireless Commun.*, vol. 13, no. 2, pp. 902–912, Feb. 2014.

[37] S. Lee, R. Zhangand K. Huang, "Opportunistic wireless energy harvesting in cognitive radio networks,"*IEEE Trans. Wireless Commun.*, vol. 12, no. 9, pp. 4788–4799, Sept. 2013.

[38] D. N. Nguyen, H. Ochi, "Two-way Cognitive DF Relaying in WSNs with Practical RF Energy Harvesting Relay Hardware,"*IEICE Trans. Commun.*, vol. E99-B, No.03, Mar. 2016.

[39] R. Ahlswede, N. Cai, S. Robert Li, R. W. Yeung,"Network information flow," *IEEE Trans. Inf. Theory,* vol. 46, no. 4, pp. 120—1216, Jul. 2000.

[40] M. Xiao, M. Skoglund, "Design of network codes for multiple-user multiple relay wireless networks," *IEEE Trans. Commun.*, vol. 60, no. 12, pp. 3755–3766, Dec. 2012.

[41] S. Ulukus , A. Yener, E. Erkip, O. Simeone, M. Zorzi, P. Grover and K. Huang, "Energy Harvesting Wireless Communications: A Review of Recent Advances," *IEEE Journal on Selected Areas Communication*, vol. 33, no. 3, March 2015.

[42] M. Ku, W. Li, Y. Chen and K. J. R. Liu, “Advances in Energy Harvesting Communications: Past, Present and Future Challenges,” *IEEE Communications Surveys and Tutorials*, vol. PP, no.99, pp. 1, Nov. 2015.

[43] L. Xiao, P. Wang, D. Niyato, D. I. Kim and Z. Han. “Wireless networks with RF energy harvesting: A contemporary survey.” *IEEE Communications Surveys and Tutorials* , vol. 17, no. 2, pp.757–789, 2015

[44] N. Shinohara, “Power without wires,” *IEEE Microwave Mag.*, vol. 12, no. 7, pp. s64–s73, 2006.

[45] H. Chen, Y. Li, J. L. Rebelatto, B F. Uchoa-Filho and B. Vucetic, “Harvest-Then-Cooperate: Wireless-Powered Cooperative Communications,” *IEEE Trans. on Signal Processing* , vol. 63, no. 7, pp. 1700–1711, Feb. 2015.

[46] S. Zhang, S. C. Liew and P. P. Lam, “Hot topic: physical-layer network coding,” *ACM Mobicom.*, pp. 358–365, 2006.

[47] D. N. K. Jayakody, J. Li, B. Chen and M. F. Flanagan, “A multilevel soft quantize- and-forward scheme for multiple access relay systems,” *IEEE Person. Indoor and Mob. Radio Commun.*, pp. 464 –468, Sept. 2014.

[48] H. Ju and R. Zhang, “Throughput maximization in wireless powered communication networks,” *IEEE Trans. Wireless Commun.*, vol. 13, no. 1, pp. 418–428, 2014

[49] L. O. Valøen and M. I. Shoesmith, “The effect of PHEV and HEV duty cycles on battery and battery pack performance,” *PHEV 2007*, pp. 4–5, Nov. 2007.

Non-exclusive licence to reproduce thesis and make thesis public

I, **Akashkumar Rajaram**
(author's name)

1. herewith grant the University of Tartu a free permit (non-exclusive licence) to:

1.1. reproduce, for the purpose of preservation and making available to the public, including for addition to the DSpace digital archives until expiry of the term of validity of the copyright, and

1.2. make available to the public via the web environment of the University of Tartu, including via the DSpace digital archives until expiry of the term of validity of the copyright,

Energy Harvesting in Cooperative Communications
(title of thesis)

supervised by
Dr. Dushantha Nalin K. Jayakody and **Dr. Vitaly Skachek**. (supervisor's name)

2. I am aware of the fact that the author retains these rights.

3. I certify that granting the non-exclusive licence does not infringe the intellectual property rights or rights arising from the Personal Data Protection Act.

Tartu 19.05.2016